JOURNAL OF QUATERNARY SCIENCE (2022) **37**(5) 884–899 ISSN 0267-8179. DOI: 10.1002/jqs.3419

JQS Journal of Quaternary Science QRA Quaternary Research Association

Late Quaternary paleoenvironmental reconstructions from sediments of Lake Emanda (Verkhoyansk Mountains, East Siberia)

ANDREI A. ANDREEV,[1,2,3]* LARISA B. NAZAROVA,[1,3] MARLENE M. LENZ,[2] THOMAS BÖHMER,[1] LUDMILA SYRYKH,[3,4] BERND WAGNER,[2] MARTIN MELLES,[2] LUDMILA A. PESTRYAKOVA[5] and ULRIKE HERZSCHUH[1,6,7]*

[1]Alfred-Wegener Institute, Helmholtz Centre for Polar and Marine Research, Research Unit Potsdam, Germany
[2]Institute of Geology and Mineralogy, University of Cologne, Germany
[3]Kazan Federal University, Russia
[4]Herzen State Pedagogical University of Russia, St, Petersburg, Russia
[5]North Eastern Federal University in Yakutsk, Yakutsk, Russia
[6]Institute of Biology and Biochemistry, University of Potsdam, Potsdam, Golm, Germany
[7]Institute of Environmental Sciences and Geography, University of Potsdam, Potsdam, Golm, Germany

Received 18 March 2021; Revised 10 February 2022; Accepted 14 February 2022

ABSTRACT: Continuous pollen and chironomid records from Lake Emanda (65°17′N, 135°45′E) provide new insights into the Late Quaternary environmental history of the Yana Highlands (Yakutia). Larch forest with shrubs (alders, pines, birches) dominated during the deposition of the lowermost sediments suggesting its Early Weichselian [Marine Isotope Stage (MIS) 5] age. Pollen- and chironomid-based climate reconstructions suggest July temperatures (T_{July}) slightly lower than modern. Gradually increasing amounts of herb pollen and cold stenotherm chironomid head capsules reflect cooler and drier environments, probably during the termination of MIS 5. T_{July} dropped to 8 °C. Mostly treeless vegetation is reconstructed during MIS 3. Tundra and steppe communities dominated during MIS 2. Shrubs became common after ~14.5 ka BP but herb-dominated habitats remained until the onset of the Holocene. Larch forests with shrub alder and dwarf birch dominated after the Holocene onset, ca. 11.7 ka BP. Decreasing amounts of shrub pollen during the Lateglacial are assigned to the Older Dryas and Younger Dryas with T_{July} ~ 7.5 °C. T_{July} increased up to 13 °C. Shrub stone pine was present after ~7.5 ka BP. The vegetation has been similar to modern since ca. 5.8 ka BP. Chironomid diversity and concentration in the sediments increased towards the present day, indicating the development of richer hydrobiological communities in response to the Holocene thermal maximum.

KEYWORDS: chironomids; environmental reconstructions; Late Quaternary; pollen

Introduction

The Verkhoyansk Mountains (Fig. 1) region is known for its extremely continental climate, with winter temperature of −67.7 °C recorded in the city of Oymyakon (Stepanova, 1958). The area is not an arctic desert, but covered predominantly by northern larch (*Larix cajanderi*) forests, except for high mountains that are dominated by prostrate herb and graminoid tundra communities that become barren at higher elevations. The southern slopes of the mountain ranges are often covered by steppe-like vegetation, as summer temperatures in the region can be as high as 30–35 °C. Annual precipitation (P_{ann}) is low (~250 mm a^{-1}). The area is probably the best modern analog of the paleoenvironmental habitats dominated in northern Eurasia during Marine Isotope Stage (MIS) 4 – MIS 2 due to the unique present-day climate conditions. Reaching up to 2389 m a.s.l. (Gerasimov, 1964), the Verkhoyansk Mts act as an important orographic, biogeographic and climatic barrier separating eastern Siberia from north-eastern Siberia.

Paleoenvironmental records demonstrate that significant climatic and vegetation differences existed in western (Yakutia) and north-eastern (Beringia) parts of East Siberia during the Late Quaternary (Anderson and Lozhkin, 2001; Andreev *et al.*, 2004, 2009, 2011; Lozhkin and Anderson, 2011; Biskaborn *et al.*, 2016). Open treeless, herb-dominated plant communities dominated East Siberia during MIS 3 and MIS 2, while some Beringian pollen assemblages attributed to MIS 3 (Anderson and Lozhkin, 2001; Lozhkin and Anderson, 2011) consist of larger amounts of arboreal pollen pointing to the possible presence of shrubs and trees in the local vegetation. It is notable that *Selaginella rupestris* (an indicator of extremely dry and cold environments) was very common in plant communities of Beringia during the Late Pleistocene as reflected in pollen records from the region (Anderson and Lozhkin, 2001) but was not as common in plant communities west of the Verkhoyansk Mts (Andreev *et al.*, 2009, 2011; Müller *et al.*, 2010). The Younger Dryas (YD) cooling is recorded in the Lateglacial records from the western part of East Siberia, but in many areas in north-eastern Siberia this cooling seems to be much weaker or negligible (Anderson *et al.*, 2002; Andreev *et al.*, 2021). Kokorowski *et al.* (2008a,b) reported spatially heterogeneous climate conditions during the YD in Beringia: cooling in southern Alaska, eastern Siberia and some parts of north-eastern Siberia; and uniform or even warmer-than-present conditions in different locations from a number of sites from central and northern Alaska, northern Siberia and northern Far East Russia.

Paleoenvironmental records from boundary areas such as the Verkhoyansk Mts can provide important data explaining the heterogeneous climate conditions in Beringia during the Late Pleistocene, and especially during the Lateglacial, when the Verkhoyansk Mts were affected only by local glaciations (Popp *et al.*, 2007; Stauch and

*Correspondence: Andrei A. Andreev and Ulrike Herzschuh, as above.
E-mail: andrej.andreev@awi.de; ulrike.herzschuh@awi.de

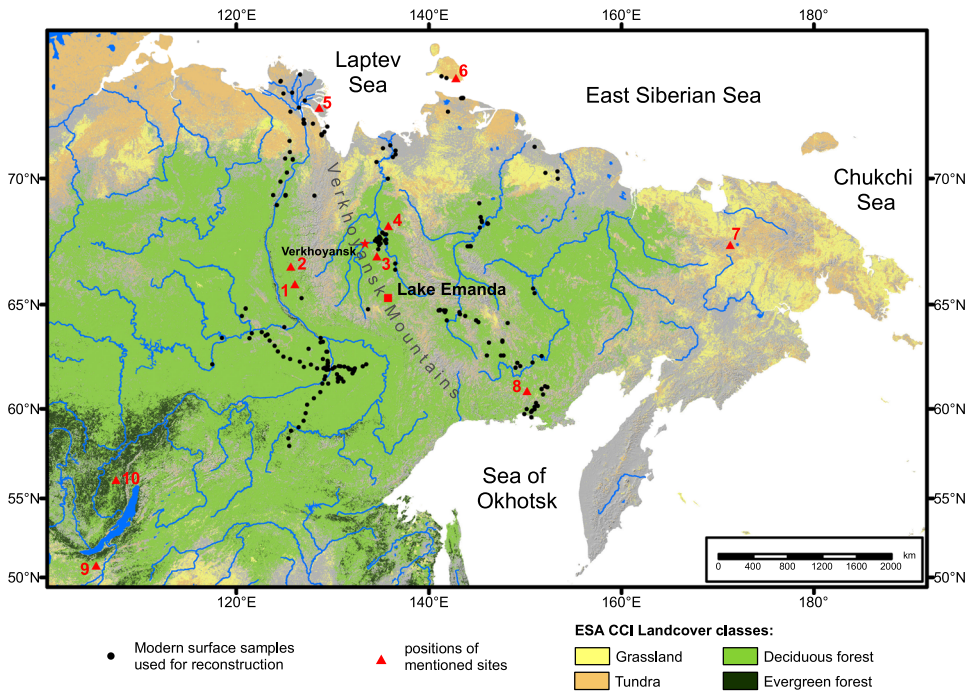

Figure 1. Location of Lake Emanda and positions of mentioned sites: 1 – Lake Billyakh (Müller *et al.*, 2010; Diekmann *et al.*, 2017); 2 – Dyanushka (Zech *et al.*, 2011); 3 – Batagay (Ashastina *et al.*, 2018); 4 – Lake Smorodinovoye (Anderson *et al.*, 2002); 5–6 – paleoenvironmental records from arctic Yakutia (Andreev *et al.*, 2002, 2009, 2011); 7 – Lake El'gygytgyn (Lozhkin *et al.*, 2006; Anderson and Lozhkin and Anderson, 2011; Melles *et al.*, 2012):); 9 – Lake Kotokel (Tarasov *et al.*, 2021); 10 – Lake Ochaul (Kobe *et al.*, 2022). [Color figure can be viewed at wileyonlinelibrary.com]

Lehmkuhl, 2010). Moreover, the Late Pleistocene and Holocene vegetation and climate history of the Verkhoyansk Mts are of particular interest as detailed reconstructions of the environmental changes, such as treeline dynamics and identification of glacial refugia for boreal trees and shrubs, are highly significant for reliable reconstructions of past climate and for validating climate and vegetation models. So far, our understanding of the palaeoenvironmental history of the area is based on a limited number of lacustrine sediment cores and permafrost ice-complex sequences, only few of which are older than the Lateglacial (Anderson *et al.*, 2002; Müller *et al.*, 2009, 2010; Zech *et al.*, 2010, 2011; Diekmann *et al.*, 2017).

Here we present a Late Quaternary paleoenvironmental record from Lake Emanda (Verkhoyansk Mts, Yakutia) that became available through the German-Russian research project PLOT (Paleolimnological Transect), which aimed to investigate the Late Quaternary environmental history of these poorly investigated continental inland areas in northern Eurasia (Melles *et al.*, 2019). In summer 2017, a 6.06-m-long sediment succession (Co1412) was recovered after a hydroacoustic survey of the lake. Lithological and geochemical studies and downward extrapolation of the ^{14}C-based sedimentation rate suggested that core Co1412 covers the last ca. 57 cal ka BP (Baumer *et al.*, 2021).

The main objective of this study is to reconstruct the Late Quaternary vegetation and climate history of the Verkhoyansk Mts based on pollen and chironomid records from core Co1412. These new environmental records allow a more precise interpretation of the sedimentological and geochemical results previously obtained from the core and provide a basis for new chronological estimations for the non-dated and/or not well-dated sediments. These new environmental records from the Verkhoyansk Mts will also complement our understanding of the climatic boundaries that existed during the Late Quaternary.

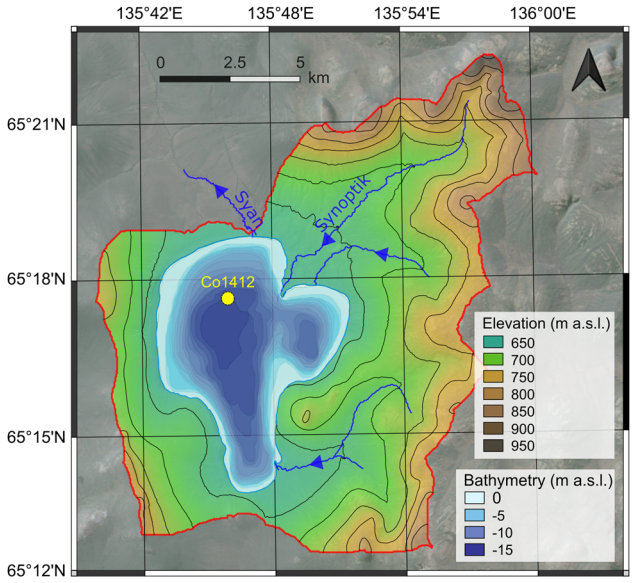

Figure 2. Topographic map of the catchment of Lake Emanda (red line) and its bathymetry. Yellow dot shows the location of sediment core Co1412. [Color figure can be viewed at wileyonlinelibrary.com]

Study site

Lake Emanda (65°17′N, 135°45′E, 671 m a.s.l) is located on the Yana Plateau in the central part of the Verkhoyansk Mts ~ 270 km south-east of the city of Verkhoyansk (Fig. 1). The heart-shaped lake is 7.5-km long, 6.5 km wide with a surface area of 33.1 km^2, maximum water depth of ~15 m and catchment of ~179 km^2 (Fig. 2; Baumer *et al.*, 2021). The main inflow, the Synoptik River, forms a delta in the north-eastern part of the lake. There are also a number of smaller creeks from the surrounding 800–1000-m-high mountains. The outflow of the lake, Syan River,

a right-hand tributary of the Derbeke River (part of the Yana River basin) drains the lake to the north.

The Triassic and Jurassic bedrock in the lake catchment predominantly consist of carbonate-bearing conglomerate, siltstone and sandstone (Dushin *et al.*, 2009). The area is a part of the Verkhoyansk–Chukotka orogenic zone formed during the Mesozoic, when the Siberian Craton collided with the Kolyma–Omolon microcontinent (Parfenov, 1991; Oxman, 2003).

The study region experiences an extremely continental climate predominantly controlled by the Siberian high-pressure system, which causes very cold and long winters, and low P_{ann}. The summer climate is mainly controlled by the Asiatic Thermal low-pressure system and a high-pressure system over the North Pacific (Barr and Clark, 2012) causing short but relatively warm summers (wcatlas.iwmi.org/results.asp). According to records from the meteorological station located on the Lake Emanda shore, local average air temperatures vary from −44.7 °C in January to 13 °C in July with an annual mean of −15.9 °C and P_{ann} reaching 250 mm with a maximum of 147 mm in summer. Moisture is mainly provided by winds from the North Atlantic, North Pacific and Arctic Ocean (Papina *et al.*, 2017).

Lake Emanda is covered by ice from early October to late May (Glushkov, 2015). The water temperature reaches 17–21 °C in summer and pH varies between 6.7 and 7.0. The lake ecosystem has limited anthropogenic influence.

Cold deciduous forests with larch (*Larix cajanderi*) dominate the study area, occupying low-elevation plains, mountain slopes and river valleys, while tundra communities cover the mountains above the treeline. Vegetation around the lake is composed of larch forest with abundant shrubs (*Betula nana*, *Alnus fruticosa*, *Pinus pumila*). Low ericaceous shrubs such as *Vaccinium vitis-idaea*, *V. uliginosum*, *Arctous alpina*, *Ledum palustre*, *Cassiope tetragona* and *Empetrum nigrum* dominate in the understory. Herbs from Poaceae, Cyperaceae, Rosaceae and Asteraceae, mosses (*Polytrichum* sp., *Dicranum* sp., *Sphagnum* sp.) and lichens are also common.

Methods

Coring

A field campaign with hydroacoustic profiling and coring was carried out during a joint Russian–German expedition in August 2017. The coring position (65°17.649′N, 135°45.554′E) was selected in the western lake basin at a water depth of 14.6 m, where the hydroacoustic data show horizontal and parallel reflectors (Fig. 2; for details see Baumer *et al.*, 2021). Coring at site Co1412 was conducted from a platform (UWITEC Ltd, Austria). Surface sediments down to 62 cm below the lake floor were recovered with a UWITEC gravity corer (Co1412-1). Sediments down to 606 cm were retrieved by a UWITEC piston corer with 50 cm overlap (for details see Baumer *et al.*, 2021). The sediment cores were collected within 3-m PVC liners, cut into pieces of ≤1 m and transported to Germany. Sediment cores were opened, split lengthwise and subsampled at the laboratory of the Institute of Geology and Mineralogy, University of Cologne. The preparation of samples for pollen and chironomid analyses was conducted at the Alfred-Wegener Institute (AWI), Research Unit Potsdam.

Radiocarbon dating

Seventeen radiocarbon dates have been retrieved from the sediment succession Co1412 (Table 1; Baumer *et al.*, 2021). Thirteen samples were sieved using a > 63-μm mesh size to find plant remains for ^{14}C dating. Different techniques were used for chemical pretreatment and graphitization of the extracted remains at the University of Cologne Center for accelerator mass spectrometry (AMS) (for details see Baumer *et al.*, 2021). Two sample aliquots (from 253.5 and 258.5 cm depths) were used for control measurement at the BETA Analytical Radiocarbon Dating Laboratory (Miami, FL, USA) after pretreatment following the standard Beta Analytical protocol. Additionally, two bulk organic samples from 345.5 and 465 cm depths were ^{14}C-dated at the BETA Laboratory. For details concerning the subsampling and the applied dating techniques see Baumer *et al.* (2021).

Table 1. Radiocarbon dates from core Co1412. Dating was performed at the University of Cologne Center for AMS dating (CologneAMS, COL) and the BETA Analytical Radiocarbon Dating Laboratory (BETA). Dating was performed on indeterminable plant remains, except for samples BETA506615 and BETA506616, were bulk organic sediment was dated. For samples with low organic content, an elementar analyser (VarioMicroCube, Elementar, Germany) was used to produce CO_2 gas directly inserted into the AMS (EA-AMS), to avoid further loss of sample material by graphitization. The IntCal13 curve (Reimer *et al.*, 2013) was used for calibration.

Sample ID	Composite depth (cm)	Dating method	C (μg)	Uncalibrated age (^{14}C a BP)	2σ confidence interval (a)	Calibrated age (cal a BP)	2σ confidence interval (a)
COL5517	51.5	EA-AMS	52	4695	167	5290	466
COL5518	98.5	EA-AMS	114	9269	285	10 190	476
COL5519	168.6	EA-AMS	94	14 592	540	17 070	663
COL5520	253.5	EA-AMS	18	19 804	1026	22 590	1113
BETA506615	253.5	AMS		27 720	140	31 440	570
COL5847	258.5	AMS	641	45 423	1480	48 900	3376
BETA528646	258.5	AMS		25 750	180	29 860	1056
COL5521	279.5	EA-AMS	61	31 375	238	35 220	1030
COL5848	286.5	AMS	303	44 198	442	47 380	2203
COL5849	306	AMS	443	45 769	363	49 300	1560
COL5522	307	EA-AMS	24	>35 000	428	>35 000	
BETA506616	345.5	AMS		32 400	220	36 280	1070
COL5850	386.5	AMS	320	39 299	321	43 040	1042
COL5851	416	AMS	733	48 128	2034	50 000	2085
COL5852	465	AMS	999	49 559	2402	*	
BETA513327	465	AMS		39 810	410	43 400	1427
COL5853	502.5	AMS	613	46 886	1762	50 000	2612

*Beyond the calibration curve.

Pollen

A standard HF technique was used for pollen preparation (Berglund and Ralska-Jasiewiczowa, 1986). One tablet of *Lycopodium* marker spores was added to each sample for calculating total pollen and spore concentration, following Stockmarr (1971). Water-free glycerol was used for sample storage and preparation of the microscopic slides. Pollen and spores were identified at a magnification of 400× with the aid of published pollen keys and atlases (Kupriyanova and Alyoshina, 1972, 1978; Bobrov *et al.*, 1983; Reille, 1992, 1995, 1998). In addition to pollen and spores, a number of non-pollen palynomorphs (NPPs; namely fungi spores, remains of algae and invertebrates) were also identified when possible and counted. These NPPs are valuable indicators of past environments (van Geel, 2001).

At least 250 pollen grains were counted in each sample. The relative frequencies of pollen taxa were calculated from the sum of the terrestrial pollen taxa. Spore percentages are based on the sum of pollen and spores. The percentages of fungi spores are based on the sum of the pollen and fungi spores, and the percentages of algae are based on the sum of pollen and algae. TGView software version 1.7.16 (Grimm, 2004) was used for calculation of percentages and for drawing the diagram (Fig. 3). The diagram was zoned by a qualitative inspection of significant changes in pollen associations, pollen concentrations and occurrence of particular indicator taxa.

Chironomids

Treatment of sediment samples for chironomid analysis followed standard techniques described in Brooks *et al.* (2007). Subsamples of wet sediments were deflocculated in 10% KOH, heated to 70 °C for 10 min by adding boiling water and left for another 20 min. The sediment was then passed through stacked 225- and 90-μm sieves. Chironomid larval head capsules were picked out of a grooved Bogorov sorting tray under a stereomicroscope at a magnification of 25–40× and were mounted in Hydromatrix two at a time, ventral side up, under a 6-mm-diameter cover slip. Chironomids were identified to the highest possible taxonomic resolution following Wiederholm (1983) and Brooks *et al.* (2007). Information on ecological preferences of identified chironomid taxa was taken from Brooks *et al.* (2007), Moller Pillot (2009, 2013) and Nazarova *et al.* (2008, 2011, 2015, 2017a). In total, 44 chironomid samples were studied. Choice of the samples depended on the availability of the material for chironomid analysis. Between 0 and 100 cm and between 320 and 606 cm we studied samples in ca. 20-cm intervals that corresponds to an average of 2000 years of sedimentation between the studied samples. Between 100 and 200 cm, we studied samples in ca. 4-cm intervals, which corresponds to ca. 350 years. Between 200 and 320 cm, we studied samples in ca. 17-cm intervals that corresponds to ca. 1650 years.

The percentage diagram (Fig. 4) was made in C2, version 1.7.7 (Juggins, 2007). Zonation of the chironomid stratigraphy was accomplished using the optimal sum-of-squares partitioning method (Birks and Gordon, 1985) using the program ZONE (Lotter and Juggins, 1991). The number of significant zones was assessed by a broken stick model (Bennett, 1996), using program the BSTICK (Birks and Line, unpublished). Effective numbers of occurrences of chironomid taxa were estimated using the N2 index (Hill, 1973). Principal components analysis (PCA) was used to explore the main pattern of taxonomic variation of chironomids throughout the sediment core (ter Braak and Prentice, 1988; Palagushkina *et al.*, 2012; Biskaborn *et al.*, 2019).

Climate reconstructions

Pollen-based climate reconstructions

Climate reconstructions are based on pollen percentages calculated according to Cao *et al.* (2013) and their taxonomic harmonization approach (only terrestrial taxa were used for calculation). A modern pollen training dataset (540 modern sites, Fig. 1) was selected within a 1000-km radius around the Lake Emanda from the Eurasian modern pollen database (EMPD) (Davis *et al.*, 2020). The modern training dataset was taxonomically harmonized similar to the fossil taxa. For all modern pollen sites, corresponding mean July temperature (T_{July}) and P_{ann} were extracted from WorldClim 2 data (Fick and Hijmans, 2017; https://www.worldclim.org/). T_{July} ranges from 3.1 to 18.7 °C and P_{ann} from 136 to 644 mm. The climate reconstructions were performed using the modern analog technique (MAT) transfer function (Overpeck *et al.*, 1985), taking seven analogs in the modern pollen training dataset into account by using the MAT-function in the *rioja* package (version 0.9-21, Juggins, 2019) for R software (R Development Core Team, 2010). In addition, a statistical significance test (Telford and Birks, 2011) was performed for the reconstruction using the randomTF-function in the *palaeoSig* package (version 2.0-3; Telford, 2019). T_{July} and P_{ann} were tested as single variables, as well as taking, respectively, the other variable as condition.

The reconstructed T_{July} and P_{ann} were plotted against depths (Fig. 5). Dissimilarity (chord distance, DC) between modern pollen assemblages and fossil pollen assemblages from Lake Emanda were calculated. Dissimilarities of fossil assemblages above the 95% confidence interval were considered to have no analogs in the modern calibration set (Overpeck *et al.*, 1985).

Chironomid-based climate reconstructions

T_{July} was inferred by using the North Russian (NR) chironomid-based temperature inference model (WA-PLS, second component; r^2 boot = 0.81; RMSEP boot = 1.43 °C). The model is based on a modern calibration dataset, which includes 193 lakes and 162 taxa from East and West Siberia (61–75°N, 50–140°E) with T_{July} ranging from 1.8 to 18.8 °C (Nazarova *et al.*, 2008, 2011, 2015). The modern T_{July} for the lakes from the calibration dataset are derived from New *et al.* (2002). The T_{July} model used was previously applied for paleoclimatic inferences and demonstrated high reliability of the reconstructed parameters (Nazarova *et al.*, 2017b, 2020; Subetto *et al.*, 2017; Syrykh *et al.*, 2017; Wetterich *et al.*, 2018). Chironomid-based reconstructions and PCA were performed in C2 version 1.7.7 (Juggins, 2007). The percentage species abundance data were square-root-transformed to stabilize species variance.

The reliability of the chironomid-inferred temperature reconstruction was assessed by several methods. The percentages of the fossil chironomid taxa that are absent or rare in the modern calibration dataset were calculated (Druzhinina *et al.*, 2020). A taxon is considered rare in the modern dataset when it has a Hill's N2 below 5 (Hill, 1973). The environmental optima of taxa that are rare in the modern dataset are likely to be poorly estimated (Brooks and Birks, 2001; Nazarova *et al.*, 2020). The MAT was performed using C2 version 1.7.7 (Juggins, 2007) with squared chord distance as the dissimilarity coefficient to determine whether the modern calibration models had adequate analogs for the fossil assemblages (Overpeck *et al.*, 1985; Nazarova *et al.*, 2013; Plikk *et al.*, 2019). Confidence intervals were based on the minimum dissimilarity coefficient distance within the

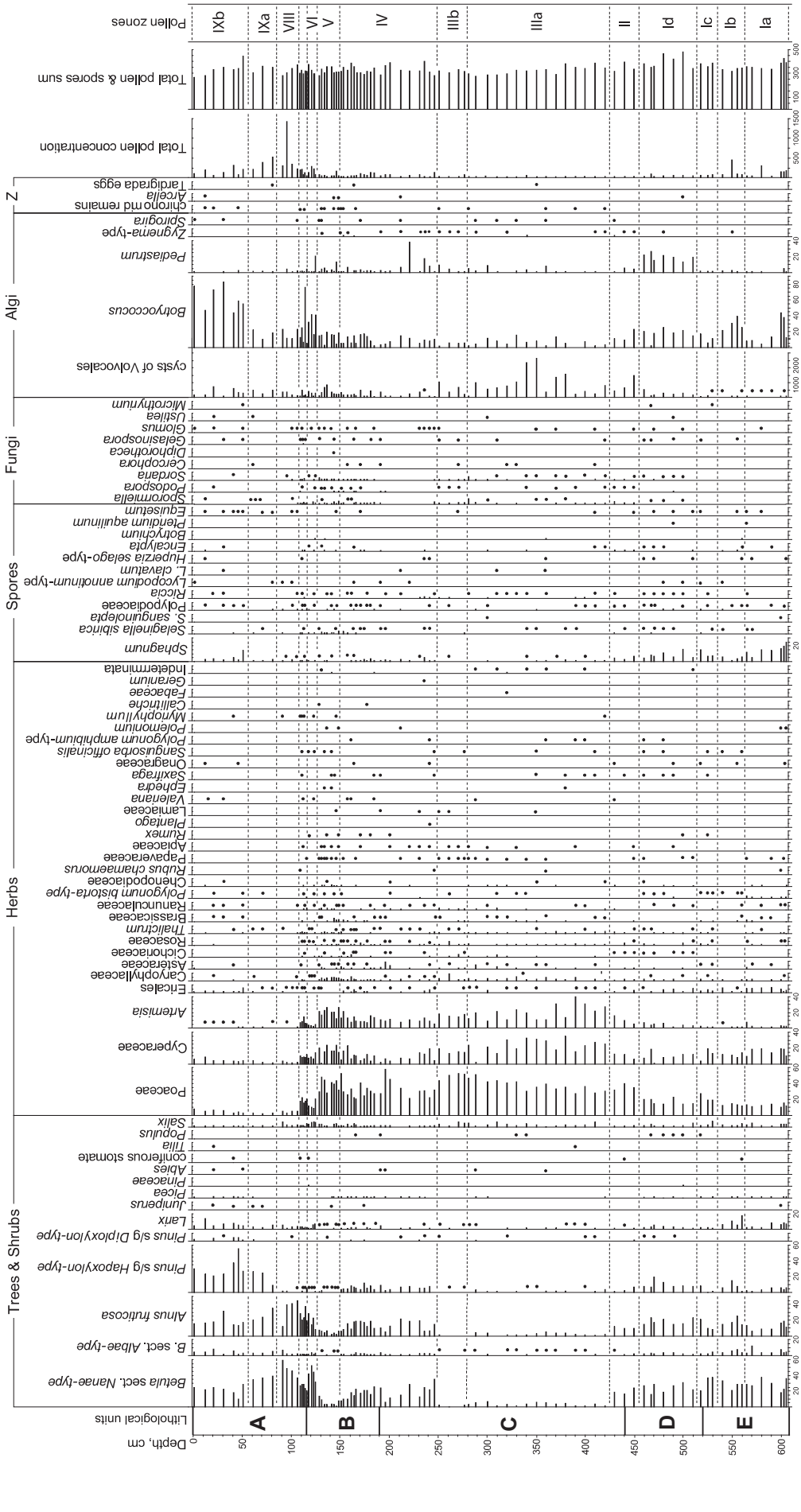

FIGURE 3 Continued.

calibration sets (Laing *et al.*, 1999). Fossil assemblages above the 95% confidence interval were considered to have no analogs in the calibration set, while assemblages with confidence interval between 75 and 95% were considered to have fair analogs (Francis *et al.*, 2006; Solovieva *et al.*, 2015; Palagushkina *et al.*, 2017). The sample scores of the first few PC axes were compared to the reconstructed temperatures. The variability of the sample scores was determined based on the first few ecological gradients of the species. Ideally, it should be dominated mainly by the variable being reconstructed (Kumke *et al.*, 2004). To find potential statistically significant relationships between species composition PCA and the inferred T_{July}, we performed an ordinary least square regression using PAST (Hammer *et al.*, 2001; Solovieva *et al.*, 2005).

Results

Core sedimentology

Core Co1412 has a composite length of 606 cm and consists of predominantly silt-dominated hemipelagic sediments. The detailed sedimentological and geochemical data were published by Baumer *et al.* (2021), who reported that sediment color and structure do not point to any distinct lithological boundaries or major hiatuses except a gap between 299 and 288-cm composite depth. This part of the core consisted of sand, which was lost during core handling on deck. Based on lithological variations the studied sediments were divided into five units: E, 606–520 cm depth; D, 520–441 cm; C, 441–189 cm; B, 189–108 cm; and A, 108–0 cm (Figs. 3 and 6, for details see Baumer *et al.*, 2021).

Core chronology

Dating of sediment samples from Lake Emanda yielded 17 ^{14}C ages ranging between 4695 ± 167 and 46 886 ± 1762 a at 51.5 and 502.5 cm depth (Table 1). The sediments below 5 m are obviously beyond the limit of the ^{14}C method and therefore cannot be directly dated. Most samples from the lower sediments (COL5847–COL5853, Table 1) demonstrate chronological inversions, which could reflect a significant contribution of old carbon from the catchment and/or possible contamination during sample preparation and processing. Some samples taken close together show differences of up to 20 000 years (Table 1) suggesting that these ages might be biased. The obviously 'too old' ^{14}C dates were excluded from the model published by Baumer *et al.* (2021), and extrapolation of sedimentation rates led to an age estimation of ca. 57 cal ka BP for the basal sediments (Fig. 6).

Pollen stratigraphy

A total 74 different pollen, spore and NPP types were found in the 89 samples studied for palynomorphs from the Emanda core. The pollen and spore assemblages (Fig. 3) were subdivided into nine main pollen zones (PZs) based on visual inspection of the diagram.

PZ I (~606–455 cm) is dominated by *Betula*, *Alnus*, *Pinus*, Poaceae and Cyperaceae pollen, *Sphagnum* spores and remains of green algae colonies (*Botryococcus*, *Pediastrum*). The zone can be subdivided into four subzones. PZ Ia (~605–562 cm) is notable by relatively high content of *Larix* and Ericales pollen. PZ Ib (~562–535 cm) demonstrates higher percentages of *Larix* and *Pinus* pollen, and remains of

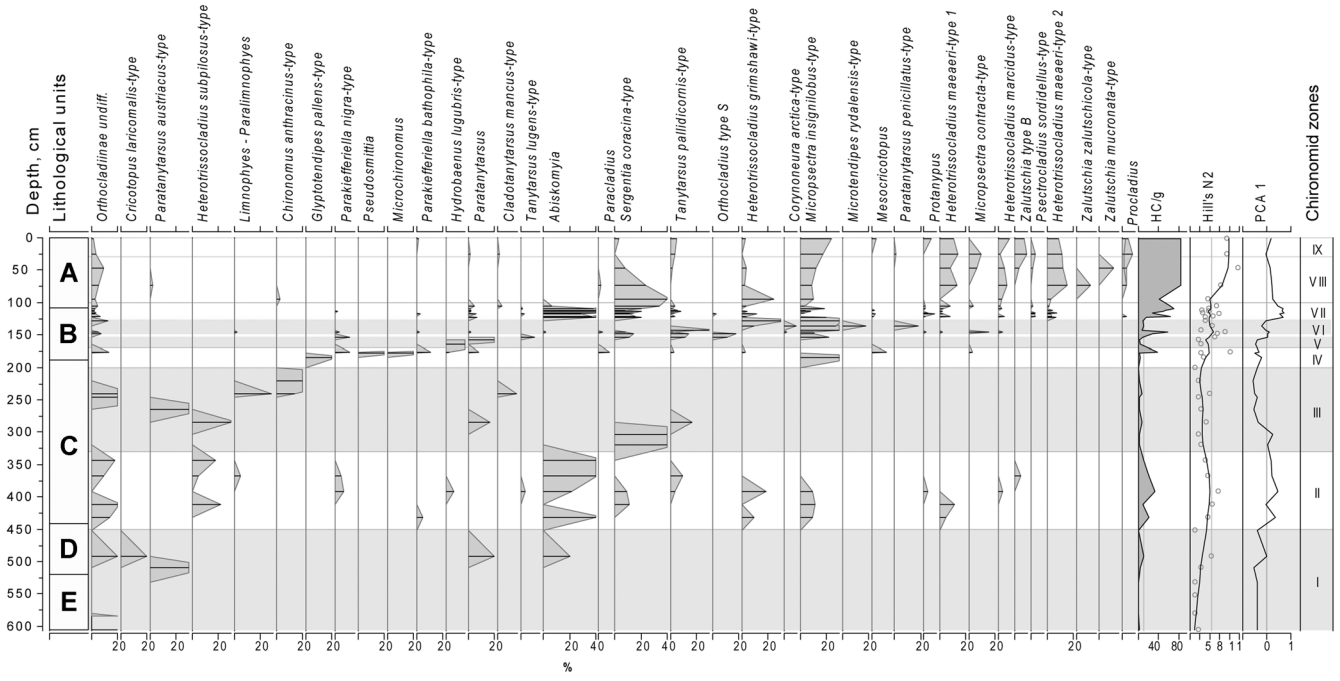

Figure 4. Relative proportions of the most abundant chironomid taxa in the Co1421 sediments from the Lake Emanda, PCA axes 1 scores for chironomid data, N2 diversity and concentration of chironomids in sediments (head capsules/g). Gray horizontal shading shows parts of the core with low concentration of chironomid head capsules. Chironomid taxa are sorted by weighted average. For lithology key see Fig. 3.

Figure 3. Percentage pollen, spore and non-pollen palynomorph diagram of the sediment core Co1421. Dots indicate that presence of taxa is <1%. Lithological units: E – brown to gray silt with relatively high clay content; D – light brown to gray silt with distinct, black lamination and relatively low clay content; C – well-layered gray silty sediments with gradual increase in sand content and the occurrence of sporadic pebbles; B – dark gray silt intervals with distinct black laminae to beige, diffusely layered intervals at 189–108 cm; and A – 108–0 cm (for details see Baumer *et al.*, 2021).

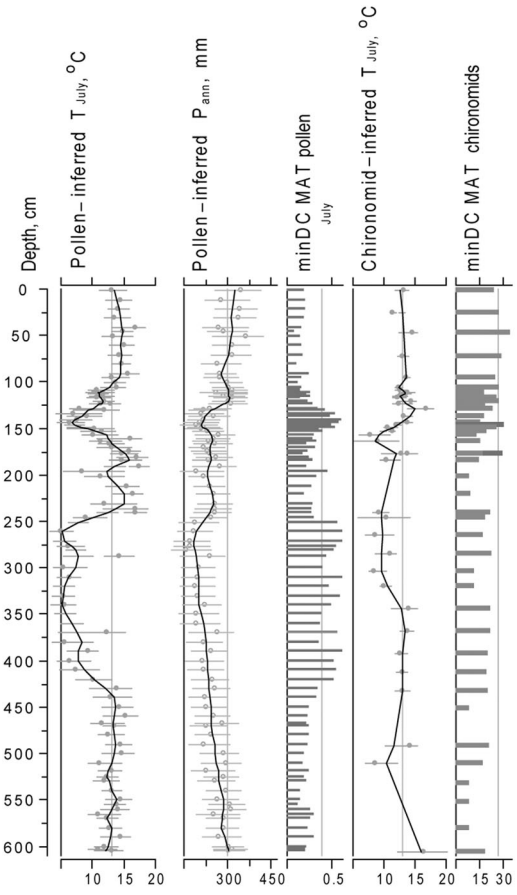

Figure 5. Reconstructed climate parameters: T_{July} and annual precipitation (P_{ann}) inferred from the pollen record using modern analog (MAT) transfer function (1000 km); chironomid-inferred T_{July}, and results of minimum dissimilarity (min DC) MAT tests for the reconstructed T_{July} and P_{ann}. For T_{July} and P_{ann}, gray vertical lines represent the modern T_{July} and P_{ann}. Gray circles with lines represent the reconstructed T_{July} and P_{ann} with error bars, and the black line represents a LOESS 0.15 smoothing of the data. The gray line for minDC MAT represents the 95% confidence interval that is considered to show no analogs with the training sets.

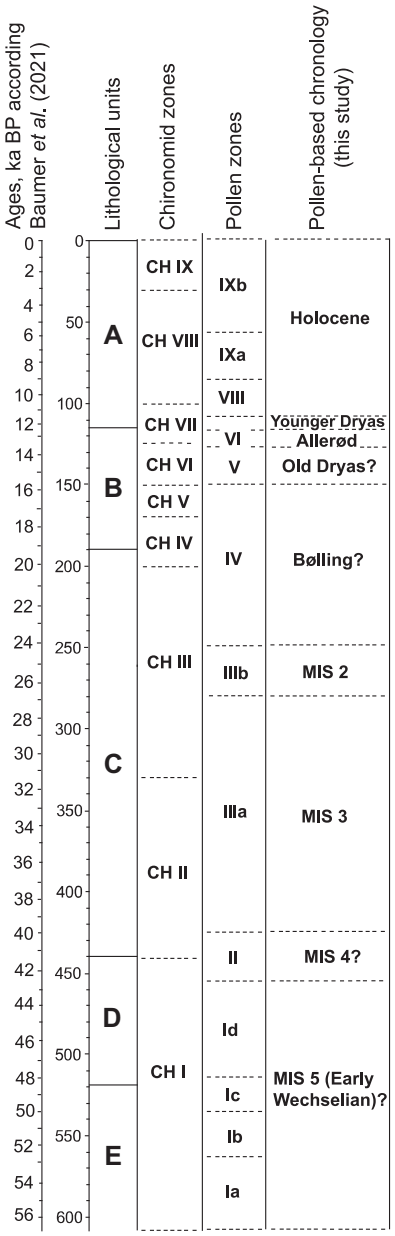

Figure 6. Age/depth model according Baumer *et al.* (2021), lithological units (for key see Fig. 3), pollen and chironomid zones and the pollen-based chronology.

Botryococcus, while the presence of Ericales pollen and *Sphagnum* spores significantly decreased. PZ Ic (~535–515 cm) is notable by decreased percentages of *Larix* and *Pinus* pollen and *Botryococcus* colonies. PZ Id (~515–455 cm) is remarkable by slightly increased percentages of pollen and numerous remains of *Pediastrum* colonies.

PZ II (~455–425 cm) demonstrates a gradual increase in *Artemisia* and Poaceae pollen percentages, while the presence of pollen of trees and shrubs, Ericales and *Sphagnum* spores gradually decrease upwards. The subzone is also characterized by a higher content of Volvocales cysts.

PZ III (~425–248 cm) is dominated by pollen of Poaceae, Cyperaceae and *Artemisia*. Volvocales cysts are rather numerous in this zone. The zone can be subdivided into two subzones. PZ IIIb (~280–248 cm) differs from PZ IIIa by absence or very low presence of *Betula* and *Alnus* pollen.

PZ IV (~248–150 cm) shows marked increases in the percentages of *Betula*, *Alnus* and *Pinus* pollen, while pollen percentages of Poaceae, Cyperaceae and *Artemisia* decreased. The pollen concentration is significantly higher than in PZ III.

PZ V (~150–125 cm) is dominated by Poaceae, Cyperaceae and *Artemisia* pollen, while pollen percentages of *Betula*, *Alnus* and *Pinus* pollen decreased.

PZ VI (~125–115 cm) is remarkable due to increased percentages of *Betula* and *Alnus* pollen and numerous remains of *Botryococcus* colonies, while pollen percentages of Poaceae, Cyperaceae and *Artemisia* decreased significantly. There is a small peak of *Larix* pollen. Pollen concentration is significantly higher than in PZ V.

PZ VII (~115–108 cm) shows a significant increase in percentages of Poaceae and *Artemisia* pollen, while pollen percentages of *Betula* decreased.

PZ VIII (~108–85 cm) is remarkable by a decrease in pollen percentages of Poaceae, Cyperaceae and *Artemisia*, while percentages of *Betula* and *Alnus* pollen increased significantly. *Larix* pollen is present in the zone, too. Pollen concentration is significantly higher than in PZ VII.

The uppermost PZ IX is dominated by *Betula*, *Alnus*, *Pinus* and *Larix* pollen. Pollen concentration is high. The zone can be subdivided into two subzones. PZ IXb (~55–0 cm) differs from PZ IXa by high content of *Larix*,

Poaceae, Cyperaceae and Ericales pollen, *Sphagnum* spores and remains of *Botryococcus*. Pollen concentration in this subzone is lower than in PZ IXa.

Pollen-based climate reconstructions

The comparison of fossil pollen spectra with the modern training dataset revealed close analogs for the spectra from the upper 120 cm of sediments and good analogs for the spectra between 606 and 450 cm, while the spectra between 450 and 120 cm revealed only poor analogs (Fig. 4). This indicates that the pollen-inferred parameters for the middle part of the core should be taken with caution.

T_{July} reconstructed from the pollen assemblages in the deepest part of the core (606–430 cm) fluctuated between 10.9 and 15.3 °C (Fig. 5). The reconstructions based on pollen assemblages show a strong temperature decrease to 4.4 °C between 430 and 250 cm. These cold climate conditions were interrupted by peaks of elevated temperatures of 12.4 and 14.3 °C in the samples from 370 and 290-cm depth, respectively. A strong T_{July} increase of 12.1 °C was reconstructed based on pollen assemblages above 250 cm depth. It reaches a maximum of 17.5 °C at 190 cm. Short cooling events were reconstructed based on pollen assemblages from the sediments at 200 cm and between 151 and 109-cm depth. T_{July} inferred from pollen spectra of the uppermost 120 cm vary between 13.2 and 16.9 °C.

P_{ann} values reconstructed from the pollen assemblages of the lower part of the core (606–280 cm) are characterized by fluctuations from 315 to 160 mm but generally show a constant decreasing trend (Fig. 5). P_{ann} values reconstructed from the upper 280 cm pollen assemblages show an increasing trend. Climate conditions became step-wise wetter again with major increases reflected at the pollen spectra from 240, 125 and 50 cm P_{ann} values reconstructed from the pollen assemblages of the uppermost 120 cm of the core fluctuated between 265 and 362 mm.

The estimated root mean squared-error of prediction (RMSEP) in our approach is derived from cross-validation of modern samples. The RMSEP resulted in 1.56 °C for T_{July} and 55.48 mm for P_{ann} on average. This indicates that the absolute values may be biased by the value of the RMSEP, but as error structure is probably strongly temporally autocorrelated, relative changes among samples contain a much lower error. This means that the climate time-series may need to be shifted to the left or right by about the RMSEP, although the relative difference can be interpreted. Trends between sections rather than fluctuations between single samples should therefore be interpreted because the MAT is sensitive to availability of analogs. The inclusion or exclusion of single modern samples during the MAT routine may artificially cause some fluctuations that may increase the already low signal-to-noise ratio of pollen data originating from the abundance changes of high pollen producers and the fact that pollen data are a 'closed' data set (i.e. percentage data where changes in one taxon affect all other taxa).

According to cross-validation results of the calibration set, the correlation (r^2) between modern and reconstructed values shows that the reconstructed T_{July} is more reliable ($r^2 = 0.76$) than P_{ann} ($r^2 = 0.47$). T_{July} as well as P_{ann} are significant as both meet the significance threshold ($p < 0.01$).

Chironomid stratigraphy

The chironomid fauna of the investigated core Co1412 includes 67 taxa (Fig. 4). Several parts of the core contain very low numbers of chironomid head capsules (HCs). Namely, HCs are rare or not found between 606 and 450 cm and between 330 and 180 cm. Hill's N2 diversity of chironomid communities varies considerably within the core (0–13.2) (Fig. 4), with the highest diversity in the upper part of the core, where the highest concentration of chironomid HCs was found.

The chironomid assemblages are subdivided into nine zones (CH I – CH IX, Fig. 4).

CH I (~606–450 cm). Chironomids were found only at 606 cm depth and between 510 and 490 cm. The assemblages are very poor (N2 < 5) and represented by oligotrophic cold-stenotherm taxa (*Abiskomyia*, *Paratanytarsus austriacus*-type) and/or eurytherm phytophilic (*Paratanytarsus*, *Cricotopus laricomalis*-type).

CH II (~450–330 cm) is dominated by cold stenotherm oligotrophic *Abiskomyia*, *Sergentia coracina*-type, *Heterotrissocladius subpilosis*-type. Three further *Heterotrissocladius* acidophilic taxa are also present: *Heterotrissocladius marcidus*-type, and *Heterotrissocladius maeaeri*-types 1 and 2. Taxonomic diversity in the zone is poor, but the concentration of HCs and N2 of chironomid communities are higher than in CH I reaching 23 HCs g^{-1} at a depth of 392 cm. Above 392 cm, the diversity of chironomid communities declines and remains low.

CH III (~330–200 cm) is characterized by low abundances of chironomid HCs and low diversity (N2 varies between 0 at 201 cm and 4.5 at 241 cm). The communities found at 320 and 304 cm depth consist of *Sergentia coracina*-type and *Tanytarsini* sp. These taxa are replaced by cold-stenotherm *Heterotrissocladius subpilosis*-type and *Paratanytarsus austriacus*-type above 285 cm. At 241 cm, where a high diversity (4.5) is observed, numerous HCs of shallow-water littoral *Limnophies–Paralimnophies* were found. HCs of typical littoral and phytophilic *Cladotanytarsus mancus*-type and eurytopic *Chironomus anthracinus*-type indicate cool conditions are also common.

CH IV (~200–170 cm) is notable by a diverse chironomid fauna (N2 increases to 10.8 at 177 cm) composed of taxa characteristic of cool oligotrophic lakes (*Parakiefferiella nigra*-type and *P. bathophila*-type, *Mesocricotopus*) and of taxa that prefer moderate climatic conditions, some of which are phytophilic or prefer detritus-rich lakes: *Glyptotendipes pallens*-type, *Microchironomus*, *Micropsectra insignilobus*-type. Semi-terrestrial *Pseudosmittia* is also present.

CH V (~170–150 cm). Chironomids are rare and the fauna is composed of cold stenotherm taxa (*Hydrobaenus lugubris*-type, *Parakiefferiella nigra*-type).

CH VI (~150–125 cm). The chironomid communities are dominated by acidophobic *M. insignilobus*-type, littoral oligotrophic *Microtendies rydalensis*-type and phytophilic *Paratanytarsus pennicillatus*-type. At the beginning of the zone (146 cm) N2 diversity is relatively high (9.2) but above this horizon, the diversity and concentration of chironomid HCs decline.

CH VII (~125–100 cm) is characterized by a dominance of the cold stenotherm *Abiskomyia* and *Sergentia coracina*-type. The abundance of acidophobic *M. insignilobus*-type starts to decrease. Several acidophilic taxa (*Heterotrissocladius*, *Psectrocladius*, *Mesocricotopus*) appear at low abundancies.

CH VIII (~100–30 cm) shows a marked increase in diversity of chironomid communities reaching the highest value (13.2) at 47 cm depth. The abundance of acidophobic *Micropsectra insignilobus*-type remains at 9–11%, while acidophilic *Heterotrissocladius* (*H. maeaeri*-types 1 and 2, *H. macridus*-type) and phytophilic *Zalutschia* taxa, characteristic of moderate climatic conditions, increase above 73 cm depth.

CH IX (~30–0 cm) is characterized by a high diversity of chironomid assemblages dominated by phytophilic *Micropsectra insignilobus*-type, several *Heterotrissocladius* taxa and meso- to euthrophic *Procladius*.

Chironomid-based climate reconstructions

All chironomid taxa in the fossil record are well represented ($N2 > 5$) in the modern training set. The MAT diagnostic has shown that chironomid communities mainly have fair analogs in the set (Fig. 5). However, five samples from the upper part of the core (25, 73, 95.5, 106 and 146 cm) show poor analogs with the training set. The first PC axis, which is the major hypothetical gradient in PCA, correlates significantly with the inferred T_{July} ($r = 0.61$, $p \leq 0.05$). The higher PC axes were not correlated with the inferred T_{July} and therefore secondary gradients cannot be explained by inferred temperature changes. The high representation of the chironomid taxa in the training set, high correlation of the inferred T_{July} with the first PC axis together with mostly good MAT results indicate that our chironomid-based temperature reconstructions from the core Co1412 record are reliable. However, the reconstructions at depths with poor analogs should be taken with caution.

T_{July} inferred from the chironomid complexes (Fig. 5) found at depths of 606 and 490 cm are above the modern (16.6 and 14.4 °C, respectively). At 510 cm depth, T_{July} is below the modern level (8.7 °C). It is close to modern at 432 cm and declines to 8.4 °C at 304 cm. Between 285 and 200 cm, the inferred T_{July} varies between 8.6 and 11.0 °C and rises thereafter. In CH IV (~200–170 cm) the reconstructed T_{July} values are 14–18 °C. Between ~170 and 150 cm, T_{July} declines (7.8–9.0 °C) and increases towards the modern level at ca. 143 cm. Between 143 and 117 cm, T_{July} values are above modern with the highest (16.7 °C) inferred at a depth of 128.5 cm. Then, the reconstructed T_{July} values vary between 12.3 °C at 117 cm and 14.4 °C at 113.5 cm. In the upper part of the core (~100–0 cm) the reconstructed T_{July} values are around the modern level (13.2–13.4 °C) with an increase (14.5 °C) at 47 cm.

Discussion

Chronological limitations

Baumer *et al.* (2021) suggested an age of ca. 57 cal ka BP for the basal sediments. Given the problematic ^{14}C ages from the studied core and its pollen stratigraphy, we suggest an alternative chronology (Fig. 6), particularly for the lower part of the record, based on pollen stratigraphy compared with dated Late Pleistocene pollen records from adjacent regions (Anderson *et al.*, 2002; Andreev *et al.*, 2002, 2009, 2011; Lozhkin *et al.*, 2006; Müller *et al.*, 2009, 2010; Zech *et al.*, 2010, 2011; Lozhkin and Anderson, 2011; Diekmann *et al.*, 2017; Tarasov *et al.*, 2021).

MIS 5?

The oldest pollen assemblages (~606–455 cm, PZ I of Fig. 3) reflect that the study area was dominated by larch forest with shrub alder and dwarf birch during the accumulation of these sediments. Pines from subgenus *Haploxylon* were also common in the vegetation. Unfortunately, it is not possible to differentiate between pollen produced by shrub stone pine (*Pinus pumila*) and Siberian pine (*Pinus sibirica*). As pollen assemblages are dominated mostly by pollen of shrub and herb taxa, we assume that *Pinus* subgenus *Haploxylon*-type pollen was produced by the relatively cold- and dry-tolerant shrub pine (*Pinus pumila*).

The pollen-based climate reconstructions show that T_{July} varied between 10.5 and 14.5 °C (Fig. 5). Chironomid-based T_{July} is 16.6 °C at the lowest depth (~606 cm) and has values of 8.7 and 14.4 °C at depths of 510 and 490 cm, respectively (Fig. 5).

High percentages of *Sphagnum* spores as well as Cyperaceae and Ericales pollen and presence of phytophilic chironomids point to wet habitats around the lake. The reconstructed P_{ann} (Fig. 5) varied between 250 and 300 mm.

It is difficult to estimate the absolute age of the PZ I interval as all ^{14}C dates, except that from 465 cm, depth are outside the dating limit (Table 1). The age model used by Baumer *et al.* (2021) suggests that sedimentation of this succession occurred between 57 and 42.6 ka BP. The pollen assemblages indicate that sediments accumulated during a warm interval with climate conditions slightly cooler or similar to the Holocene, with slightly cooler and drier conditions in the younger part of the PZ I interval. The rather high reconstructed T_{July} (Fig. 5) and interglacial character of the pollen spectra indicate that the PZ I sediments may be significantly older than the MIS 3 age suggested by Baumer *et al.* (2021), with respect to other pollen records from the surroundings. The only core containing a continuous, non-interrupted and relatively well-dated Late Pleistocene pollen record is from Lake El'gygytgyn situated ~1300 km to the north-east of Lake Emanda (Lozhkin and Anderson, 2011; Melles *et al.*, 2012). The El'gygytgyn and Emanda records show similar changes in percentages of main pollen taxa, reflecting similar environmental changes for the interval, which is reliably dated in Lake El'gygytgyn to the end of MIS 5 (Lozhkin and Anderson, 2011; Melles *et al.*, 2012).

Other existing pollen records from the region reflect much colder and drier environmental conditions during MIS 3. The most closely situated pollen record from Lake Billyakh (~420 km, Müller *et al.*, 2010; Diekmann *et al.*, 2017) shows that open herb-dominated, treeless vegetation formed the western part of the Verkhoyansk Mts between 50.7 and 13.5 ka BP, except some intervals between 40 and 32 ka BP when dwarf birches were more common.

Ashastina *et al.* (2017, 2018) reconstructed for the MIS 3 interval a meadow-steppe vegetation with inclusions of tundra-steppe taxa, and mostly dry and exposed ground in the Batagay study area (~260 km north of Emanda). Pollen spectra from the Batagay permafrost sediments, ^{14}C- and optically stimulated luminescence (OSL)-dated to 58–37 ka BP, also suggest cold climate conditions and treeless vegetation during MIS 3 (Courtin *et al.*, in press). By contrast, the macrofossil data from the OSL-dated Batagay sediments reflect that open, herb-rich northern taiga with larches, birches, shrub alders, steppe and ruderal herbs dominated the vegetation during MIS 5 (Ashastina *et al.*, 2018).

Paleoenvironmental records from arctic Yakutia (~1100 km to the north, Andreev *et al.*, 2011) reflect harsh treeless environments during MIS 3. Numerous pollen records from north-eastern Siberia (West Beringia) also suggest that treeless vegetation dominated during MIS 3 (Lozhkin and Anderson, 2011). However, there are a number of pollen records from West Beringia that contain larger amounts of shrub pollen (Anderson and Lozhkin, 2001; Lozhkin and Anderson, 2011). These assemblages were attributed to MIS 3 based on their stratigraphic position below relatively well-dated MIS 2 sediments. However, all records with relatively high percentages of shrub and tree pollen taxa are situated quite close to the Pacific coast, and therefore were more intensively influenced by maritime climate conditions in comparison to the inland areas of Beringia.

Given the high percentages of shrub and tree pollen in the lowermost sediments and the existing MIS 3 and MIS 5 pollen records from East Siberia and West Beringia, the PZ I interval reflects rather warm environmental conditions and therefore does not match climate conditions as known from the region for the period 57–42.6 ka BP. The mixed character of the pollen assemblages with relatively large amounts of shrub and herb pollen types points to the end of interglacial conditions with progressive climate cooling. The best candidate for this period is the end of MIS 5, the Early Weichselian.

The lowermost pollen spectra (PZ Ia, ~606–562 cm) reflect that larch forest with shrub alders, dwarf birches and dwarf pines in the understory dominate around the lake. *Sphagnum* and ericaceous taxa were also common in the vegetation cover, pointing to wet habitats near the lake.

The presence of numerous *Botryococcus* remains in PZ Ia sediments point to shallow-water conditions at the coring location. The phytophilic chironomid fauna (*Paratanytarsus* taxa and *Cricotopus laricomalis*-type) also reflect littoral shallow-water habitats. The diffusely layered to massive sediment appearance and overall low Mn/Fe in lithological Unit E also point to a relatively low lake level during this interval (Baumer *et al.*, 2021). We assume that the lake during the PZ Ia interval was probably much smaller and shallower than modern Lake Emanda.

The increase of *Pinus*, *Larix* and *Alnus* pollen percentages in PZ Ib (~562–535 cm) points to some warming with T_{July} up to 14 °C (Fig. 5). Lower amounts of Ericales pollen and *Sphagnum* spores reflect drier soil conditions around the lake, which may also reflect lower lake levels during the PZ Ib interval. The reconstructed P_{ann} show a significant decrease upwards during this interval that coincides with the lower clastic input revealed in sedimentological data (Baumer *et al.*, 2021). Increased amounts of *Botryococcus* remains also point to more shallow-water habitats in the lake.

The PZ Ic (~535–515 cm) interval shows a decrease of coniferous trees in the study area reflecting cooling with pollen-inferred T_{July} as low as 11 °C and chironomid-inferred T_{July} even lower (8.7 °C). Although low chironomid abundancies suggest that the T_{July} reconstruction should be taken with caution, the two reconstructions are in good accordance. Decreased presence of *Botryococcus* in the PZ Ic sediments may reflect a higher lake level in accordance with wetter soil conditions (increase in Cyperaceae and *Sphagnum*) around the lake.

PZ Id (~515–455 cm) pollen spectra show a slight increase in coniferous species and alder in the local vegetation, reflecting slight warming. PZ Ie sediments probably accumulated during a period of warming at the end of MIS 5. Pollen-based T_{July} varied greatly, reaching 15 °C (Fig. 5). Chironomid-inferred T_{July} values are in good agreement (up to 14.4 °C, Fig. 5). Numerous remains of green algae (*Pediastrum*, *Botryococcus*) colonies in the sediments point to a lower lake level at this time.

MIS 4?

PZ II (~455–425 cm) pollen assemblages show a gradual increase of mostly treeless landscapes pointing to a significant cooling with T_{July} as low as 8 °C. Lower ericaceous pollen and *Sphagnum* spore percentages reflect drier soil conditions around the lake. Higher contents of Volvocales cysts (probably produced by so-called snow algae) in the sediments may reflect a longer duration of snow and ice cover on the lake during spring. The chironomid assemblages are poor and dominated by cold stenotherm oligotrophic taxa (Fig. 4). Chironomid-based T_{July} values are close to modern at in lower part of PZ II sediments but demonstrate cooling upwards (Fig. 5).

Based on the comparison with the El'gygytgyn pollen datasets (Lozhkin *et al.*, 2006; Lozhkin and Anderson, 2011), which demonstrate the disappearance of arboreal pollen taxa, we suggest that the PZ II interval, showing gradual cooling, may coincide with the beginning of MIS 4. A more precise age estimation for this interval is complicated as the Emanda MIS 4 sediments may be not complete due the extremely low sedimentation and/or a possible hiatus. Alternatively, the PZ II interval, reflecting a gradual increase of drier and colder climate conditions, may have occurred at the termination phase of MIS 5.

Ashastina *et al.* (2018) state that meadow-steppe communities with interlocked tundra-steppe patches and scattered woodland dominated the Batagay area during MIS 4. This is similar to vegetation patterns inferred from the upper part our PZ II, but unfortunately, the Batagay permafrost records are not continuous, and only one pollen sample from MIS 4 sediments was studied there.

MIS 3

PZ IIIa (~425–280 cm) pollen spectra reflect predominantly treeless tundra- and steppe-like vegetation around the lake. However, some dwarf birch, shrub alder and willow stands probably survived in more protected habitats. The highest presence of snow algae cysts (Volvocales) in the PZ IIIa sediments may reflect longer duration of snow and ice cover on the lake during spring. Pollen assemblages points to cold and dry climate with T_{July} around 7–9 °C and P_{ann} below 250 mm (Fig. 5). Cold stenotherm oligotrophic taxa dominate the chironomid assemblages in the lower part of PZ IIIa sediments (Fig. 4). Their diversity declines upwards interval. The chironomid-based T_{July} is at modern values at the beginning of PZ IIIa (13 °C) and gradually declines to 8.3 °C at 304 cm. A cold and dry climate is also confirmed by geochemical [total organic carbon (TOC), TOC/total nitrogen (TN), $\delta^{13}C$, K/Ti] proxies (Baumer *et al.*, 2021). The pronounced coarsening of the sediments suggests a significant lake level lowering at this time.

According to the age model suggested by Baumer *et al.* (2021) the PZ IIIa sediments accumulated during MIS 3, between ca. 39.9 and 26.8 cal ka BP. Nevertheless, AMS ^{14}C dates of 50 000 ± 2085 and 35 220 ± 1030 cal a BP from 416 and 279.5 cm depth, respectively, suggest that the PZ IIIa sediments accumulated between 50 and 35 cal ka BP. The PZ IIIa pollen assemblages are in a good accordance with the high-resolution, 50-ka pollen record from Lake Billyakh (~420 km to the west; Fig. 1; Müller *et al.*, 2010). The moderate percentages of *Betula* and *Alnus* pollen in the Emanda sediments that accumulated between ca. 425 and 280 cm suggest that some shrub alders and dwarf birches grew around the lake during the sediment accumulation. The Billyakh pollen data also point to the presence of shrubs, and even larches, but generally treeless landscapes between 50.7 and 30 ka BP (Müller *et al.*, 2010), thus pre-dating the ^{14}C-based chronology of the Emanda core (Baumer *et al.*, 2021) in this interval. Based on plant macrofossil remains, Ashastina *et al.* (2018) reconstructed for the MIS 3 interval meadow-steppe vegetation with inclusions of tundra-steppe taxa, mostly dry and exposed ground in the Batagay study area. Pollen assemblages from Batagay permafrost sediments ^{14}C- and OSL-dated to 37–58-ka BP suggest cold climate conditions and treeless vegetation during MIS 3 as well (Courtin *et al.*, in press).

Ice-complex records from coastal areas of the Laptev Sea (~1100 km to the north) indicate climatic conditions comparable to full glacial times, with some fluctuations from colder/drier to slightly warmer/moister conditions during MIS 3 as well (Andreev *et al.*, 2009, 2011). Similar environmental changes are also recorded in Lake El'gygytgyn sediments (Lozhkin *et al.*, 2006; Lozhkin and Anderson, 2011). It is notable that pollen assemblages attributed to MIS 3 from the Beringian sites (namely Elikchan and Alut lakes) demonstrate larger amounts of shrub pollen (Anderson and Lozhkin, 2001; Lozhkin and Anderson, 2011). The higher presence of shrubs and trees around these sites points to slightly more favorable climate conditions in regions influenced by maritime climate conditions. Based on the AMS dates from the Emanda core and given the existing regional environmental records, we suggest an MIS 3 age, ~60–30 ka BP, for the PZ IIIa sediments.

MIS 2

PZ IIIb (~280–248 cm) sediments dominated by pollen of Poaceae, Cyperaceae and *Artemisia* reflect treeless tundra- and steppe-like habitats around the lake. Reconstructed climate variables indicate the coldest and driest climate during this interval: pollen-inferred T_{July} dropped to 7 °C and P_{ann} was slightly above 200 mm, and chironomid-inferred T_{July} was 8.6–10.4 °C (Fig. 5). The ^{14}C date, 22 590 ± 1113 cal a BP, from 253.5 cm depth, suggests that PZ IIIb sediments accumulated during MIS 2. Harsh environmental conditions recorded at our site during this time are in good accordance with MIS 2 paleoenvironmental records from adjacent regions (Anderson *et al.*, 2002; Andreev *et al.*, 2002, 2011, 2021; Müller *et al.*, 2010; Lozhkin and Anderson, 2011; Kobe *et al.*, this issue). The Billyakh record documents a lake-level lowering and strong eolian input reflecting the coldest and driest conditions recorded after 30 ka BP (Müller *et al.*, 2010; Diekmann *et al.*, 2017).

Bølling interstadial?

It remains unclear if there is a hiatus between PZ IIIb and PZ IV sediments (248 cm). Though sediment color and structure do not point to any distinct lithological boundaries or major hiatuses, the sharp changes in pollen and chironomid records above 248 cm depth suggest a hiatus or extremely low sedimentation rate during the Last Glacial Maximum (LGM). In the Lake Billyakh record, the sedimentation rate was extremely low between ca. 22 and 15 ka BP (Müller *et al.*, 2010).

According to the age model suggested by Baumer *et al.* (2021), the well-layered or distinctly laminated sandy sediments accumulated between ca. 24 and 15.7 cal ka BP. Pollen assemblages suggest that shrubs became broadly distributed near the lake at the beginning of PZ IV (~248–150 cm). However, pollen records from adjacent regions reflect that such a drastic increase in shrub taxa pollen percentages are younger than 24 cal ka BP: dated to ~13.5 cal ka BP in Lake Billyakh (Müller *et al.*, 2010), to ~12.5 cal ka BP in Lake Smorodinovoye (Anderson *et al.*, 2002), to ~13 cal ka BP in permafrost sediments from the arctic coast in Yakutia (Andreev *et al.*, 2011), and to ~14–14.5 cal ka BP in Chukotka (Lozhkin and Anderson, 2011; Andreev *et al.*, 2021). An increase in *Picea* along with an increase in shrub pollen taxa occurs at ca. 14.5 cal ka BP is seen in the Lake Kotokel sediments (Tarasov *et al.*, 2021). Based on comparison with these relatively well-dated pollen records, the drastic increase in shrub pollen in the Emanda sediments suggests deposition not much older than 14 ka BP.

Pollen-based T_{July} during the PZ IV interval varies between 12 and 14 °C, while P_{ann} varies between 250 and 280 mm (Fig. 5). We assume that this interval coincides with the beginning of significant warming at the Lateglacial in eastern and north-eastern Siberia (Andreev *et al.*, 1997, 2011, 2021; Anderson *et al.*, 2002; Müller *et al.*, 2009, 2010; Lozhkin and Anderson, 2011). This probably coincides with onset of the Bølling interstadial at ca. 14.7 ka BP.

Chironomid assemblages above 246 cm depth also indicate significant environmental changes in Lake Emanda. The assemblages are dominated by semi-terrestrial *Limnophies–Paralimnophies*, which point to increased erosion, and by *Chironomus anthracinus*-type, which is known as an early colonizer after significant environmental change (Brooks *et al.*, 2007). The typical littoral and phytophilic *Cladotanytarsus mancus*-type was also found in the sediments. Generally, the chironomid fauna suggests the appearance of wetter habitats around the lake and probably presence of macrophytes in the lake. Chironomid-based T_{July} values show an increase from 10.4 to 13.8 °C (Fig. 5).

Numerous remains of *Botryococcus* and *Pediastrum* preferring shallow aquatic habitats are in a good accordance with the chironomid data. Based on hydroacoustic data, Baumer *et al.* (2021) also suggest a lake level ~7 m lower than today during the accumulation of sediments at ~190 cm depth. The lake level drop could even have led to fluvial incisions or ice-wedge polygons forming during shallow-water conditions or seasonal, subaerial exposure. Fluctuations in total inorganic carbon, sand and the occurrence of scattered pebbles point to highly variable input from the inlet streams (Baumer *et al.*, 2021).

The sharp decrease in sand content above 189 cm depth probably indicates an increase in lake level (Baumer *et al.*, 2021). The chironomid fauna became diverse (CH IV of Fig. 4), consisting of cold oligotrophic taxa and phytophilic taxa preferring moderate conditions and detritus-rich lakes. The species composition points to littoral habitats and higher temperatures. Higher in-lake productivity is also indicated by the distinct TOC increase (Baumer *et al.*, 2021), rise of chironomid HC concentration and numerous *Botryococcus* remains. The relatively low TOC/TN suggests that aquatic productivity was relatively high, presumably due to a higher nutrient flux to the lake, increased summer temperatures and longer ice-free growing seasons. The repeated color changes in the PZ IV interval indicate distinct changes in the environmental conditions with warmer and/or wetter conditions during the sediment accumulation between 190 and 157.5-cm depth (Baumer *et al.*, 2021). At 157 cm, (CH V) chironomids are again rare in the sediments. The cold stenotherm *Hydrobaenus lugubris*-type (characteristic for wet floodplains) and *Parakiefferiella nigra*-type (characteristic for littorals of oligotrophic lakes) taxa indicate an increase in lake level (Walker *et al.*, 1992).

Old Dryas?

PZ V (~148–125 cm) is an interval with vegetation dominated by Poaceae, Cyperaceae and *Artemisia*, while shrub (*Betula*, *Alnus*, *Pinus*) stands decreased significantly from the vegetation cover, reflecting significant cooling during this time. The shrub stone pine probably completely disappeared in the study area. Both pollen- and chironomid-based T_{July} reconstructions revealed cooling culminating with a slight time lag and difference in the reconstructed absolute values. Pollen-based T_{July} is lowest between 148 and 141 cm (it dropped to 7.5 °C and P_{ann} to 210–220 mm; Fig. 5), while the chironomid-inferred T_{July} is

lowest at ca. 157 cm (7.7 °C) and is only ca. 2.5 °C below modern at 148 cm. This time lag can be explained by a slower response of the vegetation to a sharp climatic change (Ammann *et al.*, 2008; Väliranta *et al.*, 2015). We assume that the revealed PZ IV cooling may coincide with the Old Dryas cooling estimated to be from 13.9 to 13.6 cal ka BP (Klitgaard-Kristensen *et al.*, 2001). If the age estimation suggested for this Lateglacial cold interval is correct, this is the first evidence of the Old Dryas cooling in Siberia.

Chironomid diversity and concentration increase above 150 cm. The chironomid fauna is dominated by littoral oligotrophic and phytophilic taxa (Fig. 4), indicating a further lake level rise.

According to Baumer *et al.* (2021), the repeated color changes in the PZ IV interval indicate cooler and/or drier conditions during the sediment accumulation between 157.5 and 139 cm, and warmer and/or wetter conditions during the sediment accumulation between 139 and 129 cm. This is in good agreemtn with changes in pollen and chironomid assemblages above 139 cm depth, which also reflect a gradual warming and wetter conditions.

Allerød interstadial

The remarkable increase of shrub pollen in PZ VI (~125–115 cm) indicate warmer climate conditions in comparison with the previous interval. The small peak of *Larix* pollen may reflect that larch grew near the lake. We assume that the PZ VI sediments accumulated during a warm interval coinciding with the Allerød interstadial (~13.6–12.9 cal ka BP). Pollen-inferred T_{July} reached 12 °C and P_{ann} varied between 260 and 300 mm (Fig. 5). The more diverse and rich chironomid communities that developed during this interval show the highest diversity (7.5) at 117 cm (Fig. 4). The chironomid-inferred T_{July} values vary between 12.3 and 14.4 °C (Fig. 5). The lithological and geochemical data show a further decrease in sand content above 119 cm, suggesting a decreased clastic input as vegetation cover in the lake catchment during this interval became denser (Baumer *et al.*, 2021). The higher lake level and denser vegetation cover resulted in lower energy depositional environments in the lake.

Younger Dryas

PZ VII (~115–108 cm) pollen assemblages show a significant increase in percentages of herb taxa, while shrubs decreased and point to colder and drier climate conditions during this time. Pollen-inferred T_{July} dropped to 11 °C, while P_{ann} remained relatively high (ca. 300 mm). The diversity of chironomid communities drops from 7.5 at 117 cm to 3.3 on average during this interval. The observed reappearance of the cold stenotherm taxa (Fig. 4) reflect cooling with T_{July} below modern (12.2 °C). This cooling can be attributed to the YD (~12.9–11.6 cal ka BP) as sediments above 108 cm depth dominated by pollen of trees and shrubs accumulated during the Holocene.

Geochemical and lithological data also indicate distinctly cooler and drier conditions during the YD (Baumer *et al.*, 2021). However, the relatively high TOC in the sediments suggests that the climate during this cooling was less severe than during the previous cold intervals, which is in a good agreement with pollen and chironomid records.

Thus, the new pollen and chironomid data confirm that the YD cooling is pronounced in the Lake Emanda sediments, as in the sediment records from sites west and north of the Verkhoyansk Mts (Andreev *et al.*, 1997, 2009, 2011; Müller *et al.*, 2009, 2010; Andreev and Tarasov, 2013) and in some sites in West Beringia (Anderson *et al.*, 2002; Melles *et al.*, 2012; Andreev *et al.*, 2012).

Holocene

The uppermost sedimentological Unit A (108–0 cm, Baumer *et al.*, 2021) consists of brownish, diffusely layered sediments with relatively high clay and very low sand contents and coincides well with the Holocene PZs. The PZ VIII (~108–85 cm, Fig. 3) pollen assemblages reflect that larch forest with shrub alder and dwarf communities were broadly distributed around the lake, while typical glacial tundra-steppe habitats completely disappeared. T_{July} might have reached 13 °C (Fig. 5). According to the age model suggested by Baumer *et al.* (2021), PZ VIII sediments accumulated during the early Holocene between 11.6 and 9.0 ka BP. A productivity peak due presumably temperatures above present indicated by the highest TOC (Baumer *et al.*, 2021) is in good agreemtn with the highest pollen concentrations in these sediments (Fig. 3). Denser vegetation cover in the lake catchment led to lower clastic input into the lake and is reflected by relatively high clay and lowest sand contents, which indicate low transport energy of inlet streams and relatively deep waters at the coring location (Baumer *et al.*, 2021). Lower contents of *Botryococcus* remains in the sediments also point to a deeper water environment in the core location. The associated decrease in runoff and water level increase in Lake Emanda is in good agreemtn with the onset of a deep-lake stage of Lake Billyakh after 12 cal ka BP (Diekmann *et al.*, 2017).

Generally, the beginning of the early Holocene warming documented by different proxies in the Emanda sediments after 11.7 ka BP is consistent with warming signals in Lake Billyakh at ~11.3 ka BP (Müller *et al.*, 2009), in the Laptev Sea region at ~11.5 cal ka BP (Andreev *et al.*, 2011) and at Lake El'gygytgyn at ~12 cal ka BP (Lozhkin *et al.*, 2006; Swann *et al.*, 2010; Melles *et al.*, 2012).

The uppermost 85 cm (PZ IX) accumulated after 9 ka BP according to the age–depth model (Baumer *et al.*, 2021). Pollen spectra document that the study area was covered by larch forest with shrub alder and dwarf birch stands. The shrub stone pine became broadly distributed in the study area after ~7.5 ka BP. The local environmental conditions became slightly wetter after 5.8 ka (higher presence of Cyperaceae, Ericales pollen and *Sphagnum* spores). Pollen-based T_{July} values were similar to present-day conditions, varying between 13 and 16 °C, while P_{ann} varied between 300 and 350 mm (Fig. 5). Highly fluctuating TOC during the last 5.2 ka also points to unstable but similar-to-present environmental conditions (Baumer *et al.*, 2021).

The diversity of chironomid communities increases strongly at the onset of the Holocene (upper part of CH VII Fig. 4) and reach the highest values around ~4.9 ka BP (47 cm). Chironomid-based T_{July} values were close to modern. The decrease in acidophobic *Micropsectra insignilobus*-type and the increase in acidophilic *Heterotrissocladius* taxa are typical of moderate conditions. Phytophilic *Zalutschia* taxa after ~7.7-ka BP can indicate spreading of macrophytes in the lake, and slightly acidic water conditions. The acidic conditions in the lake could have been caused by decomposition of macrophytes and submerged vegetation in the lake and the paludification of the lakeshores (Moore, 1989; Nazarova *et al.*, 2017b). The paludification is also evident by an increase in wet ericaceous and *Sphagnum* habitats in the study area. By contrast, these changes also coincide with the appearance of *Pinus pumila* pollen in the sediments and probably reflect that stone pine immigrated to the study area and became common

in larch forests, which could also have led to an influx of naturally formed acids in the lake (Laing *et al.*, 1999; Nazarova *et al.*, 2017b).

The highest values of *Botryococcus* remains in the upper 50 cm of the sediments (PZ IXb) probably reflect shallow aquatic environments after 5.2 ka BP. The uppermost chironomid assemblages (CH IX, Fig. 4) dominated by phytophilic and meso- to euthrophic taxa also point to shallow water environments and lake eutrophication.

Conclusions

Micropaleontological investigations of the 606-cm-long sediment core (Co1412) from Lake Emanda provide new insights into the Late Quaternary environmental history of the Verkhoyansk area.

The pollen assemblages from basal sediments of core Co1412 document that larch forest with shrub alders, shrub stone pines and dwarf birches dominated the study area. The pollen- and chironomid-based T_{July} reconstructions indicate an interglacial climate similar to modern (up to 14.5 °C). The increased amounts of herb pollen and cold stenotherm chironomids reflect progressive cooling and the end of the interglacial phase. The absolute age of these sediments cannot be determined due the limit of the ^{14}C method, but pollen data suggest an Early Weichselian (end of MIS 5) age of the sediments.

An interval reflecting a further gradual increase of herb-dominated open landscapes and a significant cooling with T_{July} dropping to 10 °C is observed, which can be attributed to MIS 4 based on the comparison with the El'gygytgyn pollen datasets.

A predominantly treeless environment with some dwarf birch, shrub alder and willow stands survived in more protected habitats around the lake during the interval coinciding with MIS 3 according to ^{14}C dates and comparison with regional pollen records. T_{July} varied mostly between 7 and 9 °C and P_{ann} reached 200–230 mm.

Open treeless tundra-steppe vegetation dominated around the lake during the coldest and driest interval with T_{July} around 7 °C and P_{ann} slightly above 200 mm, attributed to the LGM.

Shrubs (*Betula*, *Alnus*, *Pinus*) became distributed near the lake during the Lateglacial, probably between 14 and 13 ka BP. Herb-dominated habitats were broadly distributed around the lake until the onset of the Holocene. The fluctuations in pollen and chironomid assemblages allow us to distinguish warmer and colder intervals, which can be attributed to the Older Dryas, Bølling–Allerød and YD.

The chironomid diversity and concentration increase after the Pleistocene/Holocene transition indicate development of rich hydrobiological communities in response to warming, a lake level rise and rising organic input to the lake.

The beginning of the early Holocene warming after 11.7 ka BP resulted in broadly distributed larch forest with shrub alder and dwarf birch around the lake, while typical glacial tundra-steppe habitats completely disappeared. Pollen spectra document that shrub stone pine migrated to the study area after ~7.5 ka BP. The vegetation became similar to modern after ca. 5.8 ka BP.

Acknowledgements. The work of A. Andreev was financed by a Glacial Legacy grant from European Research Council Consolidator Grant 2018-2023 and was partly supported by a Russian Scientific Foundation Grant (RSF; grant no. 20-17-00135). L. Nazarova was supported by a Russian Scientific Foundation Grant (RSF; grant no. 20-17-00135). The work of L. Pestryakova was supported by the Russian Ministry of Education and Science (grant no. FSRG2020-0019). Financial support for sediment core collection and data analyses in the scope of the PLOT and PLOT-Synthesis Projects was provided by the German Federal Ministry of Education and Research (BMBF; grant no. 03G0859A, 03F0830A). We would like to acknowledge two anonymous reviewers for their valuable comments and suggestions on earlier versions of the manuscript. Open Access funding enabled and organized by Projekt DEAL.

Data availability statement

The proxy data of core Co1412 that support the findings of this study will be available in the Pangea data repository after publication.

Abbreviations. HC, head capsule; MAT, modern analog technique; NPP, non-pollen palynomorph; PCA, principal components analysis; PZ, pollen zone; RMSEP, root mean squared-error of prediction; YD, Younger Dryas.

References

Ammann B, Eicher U, Schwander J *et al.* 2008. Biotic response to rapid climatic changes during the Late Glacial: high resolution biostratigraphies and biological processes. *Geographica Helvetica* **63**: 160–166. https://doi.org/10.5194/gh-63-160-2008

Anderson PM, Lozhkin AV, Brubaker LB. 2002. Implications of a 24,000-yr palynological record for a Younger Dryas cooling and for boreal forest development in northeastern Siberia. *Quaternary Research* **57**: 325–333. https://doi.org/10.1006/qres.2002.2321

Anderson PM, Lozhkin AV. 2001. The Stage 3 interstadial complex (Karginskii/middle Wisconsinan interval) of Beringia: variations in paleoenvironments and implications for paleoclimatic interpretations. *Quaternary Science Reviews* **20**: 93–125. https://doi.org/10.1016/S0277-3791(00)00129-3

Andreev AA, Grosse G, Schirrmeister L *et al.* 2004. Late Saalian and Eemian palaeoenvironmental history of the Bol'shoy Lyakhovsky Island (Laptev Sea region, Arctic Siberia). *Boreas* **33**: 319–348. https://doi.org/10.1080/03009480410001974

Andreev AA, Grosse G, Schirrmeister L *et al.* 2009. Weichselian and Holocene palaeoenvironmental history of the Bol'shoy Lyakhovsky Island, New Siberian Archipelago, Arctic Siberia. *Boreas* **38**: 72–110. https://doi.org/10.1111/j.1502-3885.2008.00039.x

Andreev AA, Klimanov VA, Sulerzhitsky LD. 1997. Younger Dryas pollen records from central and southern Yakutia. *Quaternary International* **41–42**: 111–117. https://doi.org/10.1016/S1040-6182(96)00042-0

Andreev AA, Morozova E, Fedorov G et al. 2012. Vegetation history of central Chukotka deduced from permafrost paleoenvironmental records of the El'gygytgyn Impact Crater. *Climate of the Past* **8**: 1287–1300.

Andreev AA, Raschke E, Biskaborn BK *et al.* 2021. Late Pleistocene to Holocene vegetation and climate changes in northwestern Chukotka (Far East Russia) deduced from lakes Ilirney and Rauchuagytgyn pollen records. *Boreas* **50**: 652–670. https://doi.org/10.1111/bor.12521

Andreev AA, Schirrmeister L, Siegert C *et al.* 2002. Paleoenvironmental changes in northeastern Siberia during the Late Quaternary – evidence from pollen records of the Bykovsky Peninsula. *Polarforschung* **70**: 13–25.

Andreev AA, Schirrmeister L, Tarasov PE *et al.* 2011. Vegetation and climate history in the Laptev Sea region (Arctic Siberia) during Late Quaternary inferred from pollen records. *Quaternary Science Reviews* **30**: 2182–2199. https://doi.org/10.1016/j.quascirev.2010.12.026

Andreev AA, Tarasov PE. 2013. Pollen records, postglacial: northern Asia. In *Encyclopedia of Quaternary Science*, Elias SA, Mock CJ (eds). Elsevier: Amsterdam; 164–172.

Ashastina K, Kuzmina S, Rudaya N *et al.* 2018. Woodlands and steppes: Pleistocene vegetation in Yakutia's most continental part recorded in the Batagay permafrost sequence. *Quaternary Science Reviews* **196**: 38–61. https://doi.org/10.1016/j.quascirev.2018.07.032

Ashastina K, Schirrmeister L, Fuchs M *et al*. 2017. Palaeoclimate characteristics in interior Siberia of MIS 6–2: first insights from the Batagay permafrost mega-thaw slump in the Yana Highlands. *Climate of the Past* **13**: 795–818. https://doi.org/10.5194/cp-13-795-2017

Barr ID, Clark CD. 2012. Late Quaternary glaciations in Far NE Russia; combining moraines, topography and chronology to assess regional and global glaciation synchrony. *Quaternary Science Reviews* **53**: 72–87. https://doi.org/10.1016/j.quascirev.2012.08.004

Baumer MM, Wagner B, Meyer H *et al*. 2021. Climatic and environmental changes in the Yana Highlands of north-eastern Siberia over the last c. 57 000 years, derived from a sediment core from Lake Emanda. *Boreas* **50**: 114–133. https://doi.org/10.1111/bor.12476

Bennett KD. 1996. Determination of the number of zones in a biostratigraphical sequence. *New Phytologist* **132**: 155–170. https://doi.org/10.1111/j.1469-8137.1996.tb04521.x [PubMed: 33863055].

Berglund BE, Ralska-Jasiewiczowa M. 1986. Pollen analysis and pollen diagrams. In *Handbook of Holocene Palaeoecology and Palaeohydrology*, Berglund BE (ed). Wiley: Chichester; 455–484.

Birks HJB, Gordon AD. 1985. The analysis of pollen stratigraphical data: zonation. In *Numerical Methods in Quaternary Pollen Analysis*, Birks HJB, Gordon AD (eds). Academic Press: London; 47–90.

Biskaborn BK, Nazarova L, Pestryakova LA *et al*. 2019. Spatial distribution of environmental indicators in surface sediments of Lake Bolshoe Toko, Yakutia, Russia. *Biogeosciences* **16**: 4023–4049. https://doi.org/10.5194/bg-16-4023-2019

Biskaborn BK, Subetto DA, Savelieva LA *et al*. 2016. Late Quaternary vegetation and lake system dynamics in north-eastern Siberia: implications for seasonal climate variability. *Quaternary Science Reviews* **147**: 406–421. https://doi.org/10.1016/j.quascirev.2015.08.014

Bobrov AE, Kupriyanova LA, Litvintseva MV *et al*. 1983. *Spores and Pollen of Gymnosperms from the Flora of the European Part of the USSR*. Nauka: Leningrad. (in Russian).

Brooks SJ, Birks HJB. 2001. Chironomid-inferred air temperatures from Lateglacial and Holocene sites in north-west Europe: progress and problems. *Quaternary Science Reviews* **20**: 1723–1741. https://doi.org/10.1016/S0277-3791(01)00038-5

Brooks SJ, Langdon PG, Heiri O. 2007. *The identification and use of Palaearctic Chironomidae larvae in palaeoecology. QRA Technical Guide No 10*. Quaternary Research Association: London.

Cao X, Ni J, Herzschuh U *et al*. 2013. A late Quaternary pollen dataset from eastern continental Asia for vegetation and climate reconstructions: set up and evaluation. *Review of Palaeobotany and Palynology* **194**: 21–37. https://doi.org/10.1016/j.revpalbo.2013.02.003

Courtin J, Perfumo A, Andreev AA *et al*. *Molecular Ecology* in press. Pleistocene glacial and interglacial ecosystems inferred from ancient DNA analyses of permafrost sediments from Batagay megaslump, east Siberia.

Davis BAS, Chevalier M, Sommer P *et al*. 2020. The Eurasian Modern Pollen Database (EMPD), version 2. *Earth System Science Data* **2**: 2423–2445.

Diekmann B, Pestryakova L, Nazarova L *et al*. 2017. Late Quaternary lake dynamics in the Verkhoyansk Mountains of Eastern Siberia: implications for climate and glaciation history. *Polarforschung* **86**: 97–110.

Druzhinina O, Kublitskiy Y, Stančikaitė M *et al*. 2020. The Late Pleistocene–Early Holocene palaeoenvironmental evolution in the SE Baltic region: a new approach based on chironomid, geochemical and isotopic data from Kamyshovoye Lake, Russia. *Boreas* **49**: 544–561. https://doi.org/10.1111/bor.12438

Dushin VA, Serdyukova OP, Malyugin AA *et al*. 2009. *State Geological Map of the Russian Federation 1: 200 000. Sheet Q42I,II*. VSEGEI: St. Petersburg. (in Russian).

Fick SE, Hijmans RJ. 2017. WorldClim 2: new 1-km spatial resolution climate surfaces for global land areas. *International Journal of Climatology* **37**: 4302–4315. https://doi.org/10.1002/joc.5086

Francis DR, Wolfe AP, Walker IR *et al*. 2006. Interglacial and Holocene temperature reconstructions based on midge remains in sediments of two lakes from Baffin Island, Nunavut, Arctic Canada. *Palaeogeography, Palaeoclimatology, Palaeoecology* **236**: 107–124. https://doi.org/10.1016/j.palaeo.2006.01.005

Gerasimov IP. 1964. *Atlas Mira*. AN SSSR-GUGK SSSR: Moscow. (in Russian).

Glushkov AV. 2015. *Rivers of Eastern Russia*. Yakutsk. (in Russian).

Grimm EC. 2004. *TGView*. Illinois State Museum, Research and Collections Center: Springfield.

Hammer Ø, Harper DAT, Raan PD. 2001. PAST: palaeontological statistics software package for education and data analysis. *Palaeontologia Electronica* **41**: 1–9.

Hill MO. 1973. Diversity and evenness: a unifying notation and its consequences. *Ecology* **54**: 427–432. https://doi.org/10.2307/1934352

Juggins S. 2007. *C2 Version 1.5 User Guide. Software for Ecological and Palaeoecological Data Analysis and Visualization*. Newcastle University: Newcastle upon Tyne.

Juggins S. 2019. rioja: analysis of Quaternary Science Data. R package version 0.9-21. https://cran.r-project.org/web/packages/rioja.

Klitgaard-Kristensen D, Sejrup HP, Haflidason H. 2001. The last 18 kyr fluctuations in Norwegian sea surface conditions and implications for the magnitude of climatic change: evidence from the North Sea. *Paleoceanography* **16**: 455–467. https://doi.org/10.1029/1999PA000495

Kobe F, Leipe C, Shchetnikov AA *et al*. 2022. Not herbs and forbs alone: pollen-based evidence for the presence of boreal trees and shrubs in Cis-Baikal (Eastern Siberia) derived from the Last Glacial Maximum sediment of Lake Ochaul. *Journal of Quaternary Science*. https://doi.org/10.1002/jqs.3290

Kokorowski HD, Anderson PM, Mock CJ *et al*. 2008a. A re-evaluation and spatial analysis of evidence for a Younger Dryas climatic reversal in Beringia. *Quaternary Science Reviews* **27**: 1710–1722. https://doi.org/10.1016/j.quascirev.2008.06.010

Kokorowski HD, Anderson PM, Sletten RS *et al*. 2008b. Late glacial and early Holocene climatic changes based on a multiproxy lacustrine sediment record from northeast Siberia. *Arctic, Antarctic, and Alpine Research* **40**: 497–505. https://doi.org/10.1657/1523-0430(07-036)[KOKOROWSKI]2.0.CO;2

Kumke T, Kienel U, Weckström J *et al*. 2004. Inferred Holocene paleotemperatures from diatoms at Lake Lama, Central Siberia. *Arctic, Antarctic, and Alpine Research* **36**: 624–634. https://doi.org/10.1657/1523-0430(2004)036[0624:IHPFDA]2.0.CO;2

Kupriyanova LA, Alyoshina LA. 1972. *Pollen and Spores of Plants from the Flora of European Part of USSR, Vol. I*. Academy of Sciences USSR, Komarov Botanical Institute: Leningrad. (in Russian).

Kupriyanova LA, Alyoshina LA. 1978. *Pollen and spores of plants from the flora of European part of USSR*. Academy of Sciences USSR, Komarov Botanical Institute: Leningrad. (in Russian).

Laing TE, Rühland KM, Smol JP. 1999. Past environmental and climatic changes related to tree-line shifts inferred from fossil diatoms from a lake near the Lena River Delta, Siberia. *Holocene* **9**: 547–557. https://doi.org/10.1191/095968399675614733

Lotter AF, Juggins S. 1991. POLPROF, TRAN and ZONE: programs for plotting, editing and zoning pollen and diatom data. *INQUA Subcommission for the study of the Holocene Working Group on Data-Handling Methods, Newsletter* **6**: 4–6.

Lozhkin AV, Anderson PM. 2011. Forest or no forest: implications of the vegetation record for climatic stability in Western Beringia during Oxygen Isotope Stage 3. *Quaternary Science Reviews* **30**: 2160–2181. https://doi.org/10.1016/j.quascirev.2010.12.022

Lozhkin AV, Anderson PM, Matrosova TV *et al*. 2006. The pollen record from El'gygytgyn Lake: implications for vegetation and climate histories of northern Chukotka since the late Middle Pleistocene. *Journal of Paleolimnology* **37**: 135–153. https://doi.org/10.1007/s10933-006-9018-5

Melles M, Brigham-Grette J, Minyuk PS *et al*. 2012. 2.8 million years of arctic climate change from lake El'gygytgyn, NE Russia. *Science* **337**: 315–320. https://doi.org/10.1126/science.1222135 [PubMed: 22722254].

Melles M, Svendsen JI, Fedorov G *et al*. 2019. Northern Eurasian lakes – late Quaternary glaciation and climate history – introduction. *Boreas* **48**: 269–272. https://doi.org/10.1111/bor.12395

Moller Pillot HKM. 2009. *Chironomidae larvae of the Netherlands and adjacent lowlands. Volume 2. Biology and Ecology of the Chironomini*. KNNV Publishing: Zeist.

Moller Pillot HKM. 2013. *Chironomidae larvae of the Netherlands and adjacent lowlands. Volume 3 Biology and Ecology of the Aquatic Orthocladiinae*. KNNV Publishing: Zeist.

Moore ML. 1989. *NALMS Management Guide for Lakes and Reservoirs*. North American Lake Management Society

Müller S, Tarasov PE, Andreev AA *et al*. 2009. Late Glacial to Holocene environments in the present-day coldest region of the Northern Hemisphere inferred from a pollen record of Lake Billyakh, Verkhoyansk Mts, NE Siberia. *Climate of the Past* **5**: 73–84. https://doi.org/10.5194/cp-5-73-2009

Müller S, Tarasov PE, Andreev AA *et al*. 2010. Late Quaternary vegetation and environments in the Verkhoyansk Mountains region (NE Asia) reconstructed from a 50-kyr fossil pollen record from Lake Billyakh. *Quaternary Science Reviews* **29**: 2071–2086. https://doi.org/10.1016/j.quascirev.2010.04.024

Nazarova L, Bleibtreu A, Hoff U *et al*. 2017b. Changes in temperature and water depth of a small mountain lake during the past 3000 years in Central Kamchatka reflected by a chironomid record. *Quaternary International* **447**: 46–58. https://doi.org/10.1016/j.quaint.2016.10.008

Nazarova L, de Hoog V, Hoff U *et al*. 2013. Late Holocene climate and environmental changes in Kamchatka inferred from the subfossil chironomid record. *Quaternary Science Reviews* **67**: 81–92. https://doi.org/10.1016/j.quascirev.2013.01.018

Nazarova L, Herzschuh U, Wetterich S *et al*. 2011. Chironomid-based inference models for estimating mean July air temperature and water depth from lakes in Yakutia, northeastern Russia. *Journal of Paleolimnology* **45**: 57–71. https://doi.org/10.1007/s10933-010-9479-4

Nazarova L, Self AE, Brooks SJ *et al*. 2015. Northern Russian chironomid-based modern summer temperature data set and inference models. *Global and Planetary Change* **134**: 10–25. https://doi.org/10.1016/j.gloplacha.2014.11.015

Nazarova L, Syrykh LS, Mayfield RJ *et al*. 2020. Palaeoecological and palaeoclimatic conditions in Karelian Isthmus (north-western Russia) during the Holocene: multi-proxy analysis of sediments from the Lake Medvedevskoe. *Quaternary Research* **95**: 65–83. https://doi.org/10.1017/qua.2019.88

Nazarova LB, Pestryakova LA, Ushnitskaya LA *et al*. 2008. Chironomids (Diptera: Chironomidae) in lakes of Central Yakutia and their indicative potential for paleoclimatic research. *Contemporary Problems of Ecology* **1**: 335–345. https://doi.org/10.1134/S1995425508030089

Nazarova LB, Self AE, Brooks SJ *et al*. 2017a. Chironomid fauna of the lakes from the Pechora River basin (east of European part of Russian Arctic): ecology and reconstruction of recent ecological changes in the region. *Contemporary Problems of Ecology* **10**: 350–362. https://doi.org/10.1134/S1995425517040059

New M, Lister D, Hulme M *et al*. 2002. A high-resolution data set of surface climate over global land areas. Data available at: wcatlas.iwmi.org. (Accessed 5 July 2020). *Climate Research* **21**: 1–25. https://doi.org/10.3354/cr021001

Overpeck JT, Webb T, Prentice IC. 1985. Quantitative interpretation of fossil pollen spectra: dissimilarity coefficients and the method of modern analogs. *Quaternary Research* **23**: 87–108. https://doi.org/10.1016/0033-5894(85)90074-2

Oxman VS. 2003. Tectonic evolution of the Mesozoic Verkhoyansk–Kolyma belt (NE Asia). *Tectonophysics* **365**: 45–76. https://doi.org/10.1016/S0040-1951(03)00064-7

Palagushkina O, Wetterich S, Biskaborn BK *et al*. 2017. Diatom records and tephra mineralogy in pingo deposits of Seward Peninsula, Alaska. *Palaeogeography, Palaeoclimatology, Palaeoecology* **479**: 1–15. https://doi.org/10.1016/j.palaeo.2017.04.006

Palagushkina OV, Nazarova LB, Wetterich S *et al*. 2012. Diatoms of modern bottom sediments in Siberian. *Arctic. Contemporary Problems of Ecology* **5**: 413–422. https://doi.org/10.1134/S1995425512040105

Papina T, Malygina N, Eirikh A *et al*. 2017. Isotopic composition and sources of atmospheric precipitation in central Yakutia. *Earth's Cryosphere* **21**: 52–61.

Parfenov LM. 1991. Tectonics of the Verkhoyansk-Kolyma Mesozoides in the context of plate tectonics. *Tectonophysics* **199**: 319–342. https://doi.org/10.1016/0040-1951(91)90177-T

Plikk A, Engels S, Luoto TP *et al*. 2019. Chironomid-based temperature reconstruction for the Eemian Interglacial (MIS 5e) at Sokli, northeast Finland. *Journal of Paleolimnology* **61**: 355–371. https://doi.org/10.1007/s10933-018-00064-y

Popp S, Belolyubsky I, Lehmkuhl F *et al*. 2007. Sediment provenance of late Quaternary morainic, fluvial and loess-like deposits in the southwestern Verkhoyansk Mountains (eastern Siberia) and implications for regional palaeoenvironmental reconstructions. *Geological Journal* **42**: 477–497. https://doi.org/10.1002/gj.1088

R Development Core Team. 2010. *A Language and Environment for Statistical Computing*. R Foundation for Statistical Computing: Vienna.

Reille M. 1992. *Pollen et spores d'Europe et d'Afrique du nord*. Laboratoire de Botanique Historique et Palynologie: Marseille.

Reille M. 1995. *Pollen et spores d'Europe et d'Afrique du nord Supplement 1*. Laboratoire de Botanique Historique et Palynologie: Marseille.

Reille M. 1998. *Pollen et spores d'Europe et d'Afrique du nord. Supplement 2*. Laboratoire de Botanique Historique et Palynologie: Marseille.

Reimer PJ, Bard E, Bayliss A *et al*. 2013. IntCal13 and Marine13 radiocarbon age calibration curves 0–50,000 years cal BP. *Radiocarbon* **55**: 1869–1887. https://doi.org/10.2458/azu_js_rc.55.16947

Solovieva N, Jones VJ, Nazarova L *et al*. 2005. Palaeolimnological evidence for recent climatic change in lakes from the northern Urals, arctic Russia. *Journal of Paleolimnology* **33**: 463–482. https://doi.org/10.1007/s10933-005-0811-3

Solovieva N, Klimaschewski A, Self AE *et al*. 2015. The Holocene environmental history of a small coastal lake on the north-eastern Kamchatka Peninsula. *Global and Planetary Change* **134**: 55–66. https://doi.org/10.1016/j.gloplacha.2015.06.010

Stauch G, Lehmkuhl F. 2010. Quaternary glaciations in the Verkhoyansk Mountains, Northeast Siberia. *Quaternary Research* **74**: 145–155. https://doi.org/10.1016/j.yqres.2010.04.003

Stepanova NA. 1958. On the lowest temperatures on earth. *Monthly Weather Review* **86**: 6–10. https://doi.org/10.1175/1520-0493(1958)086<0006:OTLTOE>2.0.CO;2

Stockmarr J. 1971. Tablets with spores used in absolute pollen analysis. *Pollen et Spores* **13**: 614–621.

Subetto DA, Nazarova LB, Pestryakova LA *et al*. 2017. Paleolimnological studies in Russian northern Eurasia: a review. *Contemporary Problems of Ecology* **10**: 327–335. https://doi.org/10.1134/S1995425517040102

Swann GEA, Leng MJ, Juschus O *et al*. 2010. A combined oxygen and silicon diatom isotope record of Late Quaternary change in Lake El'gygytgyn, North East Siberia. *Quaternary Science Reviews* **29**: 774–786. https://doi.org/10.1016/j.quascirev.2009.11.024

Syrykh LS, Nazarova LB, Herzschuh U *et al*. 2017. Reconstruction of palaeoecological and palaeoclimatic conditions of the Holocene in the south of the Taimyr according to an analysis of lake sediments. *Contemporary Problems of Ecology* **10**: 363–369. https://doi.org/10.1134/S1995425517040114

Tarasov PE, Leipe C, Wagner M. 2021. Environments during the spread of anatomically modern humans across northern Asia 50–10 cal kyr BP: what do we know and what would we like to know? *Quaternary International* **596**: 155–170. https://doi.org/10.1016/j.quaint.2020.10.030

Telford R. 2019. palaeoSig: significance tests for palaeoenvironmental reconstructions. *R package version* **2**: 0–3. https://cran.r-project.org/web/packages/palaeoSig

Telford RJ, Birks HJB. 2011. A novel method for assessing the statistical significance of quantitative reconstructions inferred from biotic assemblages. *Quaternary Science Reviews* **30**: 1272–1278. https://doi.org/10.1016/j.quascirev.2011.03.002

ter Braak CJF, Prentice IC. 1988. A theory of gradient analysis. *Advances in Ecological Research* **18**: 271–317. https://doi.org/10.1016/S0065-2504(08)60183-X

van Geel B. 2001. Non-pollen palynomorphs. In *Tracking Environmental Change using Lake Sediments. Terrestrial, Algal and Silicaceous Indicators*, Smol JP, Birks HJB, Last WM, Bradley RS, Alverson K. (eds). Kluwer: Dordrecht; 99–119.

Väliranta M, Salonen JS, Heikkilä M *et al*. 2015. Plant macrofossil evidence for an early onset of the Holocene summer thermal maximum in northernmost Europe. *Nature Communications* **6**: 6809. https://doi.org/10.1038/ncomms7809 [PubMed: 25858780].

Walker IR, Oliver DR, Dillon ME. 1992. The larva and habitat of *Parakiefferiella nigra* Brundin (Diptera: Chironomidae). *Netherlands Journal of Aquatic Ecology* **26**: 527–531. https://doi.org/10.1007/BF02255286

Wetterich S, Schirrmeister L, Nazarova L *et al*. 2018. Holocene thermokarst and pingo development in the Kolyma Lowland (NE Siberia). *Permafrost and Periglacial Processes* **29**: 182–198. https://doi.org/10.1002/ppp.1979

Wiederholm T. 1983. Chironomidae of the Holarctic region, keys and diagnoses. Part 1 *Larvae*. *Entomologica Scandinavica* **19**: 1–457.

Zech M, Andreev A, Zech R *et al*. 2010. Quaternary vegetation changes derived from a permafrost palaeosol sequence in NE-Siberia using alkane biomarker and pollen analyses: contradicting vegetation history versus climate history? *Boreas* **39**: 540–550.

Zech W, Zech R, Zech M *et al*. 2011. Obliquity forcing of Quaternary glaciation and environmental changes in NE Siberia. *Quaternary International* **234**: 133–145. https://doi.org/10.1016/j.quaint.2010.04.016

